

Design Optimization of Latent Heat Thermal Energy Storage System Using Computational Fluid Dynamics, Response Surface Methodology and Genetic Algorithm

by

Saurabh Mahadeo Mali

**A thesis submitted in partial fulfillment
of the requirements for the degree of
Master of Science in Engineering
(Mechanical Engineering)
in the University of Michigan-Dearborn
2018**

Master's Thesis Committee:

**Professor Subrata Sengupta, Chair
Professor Armen Zakarian
Professor Oleg Zikanov**

© Saurabh Mahadeo Mali

2018

Acknowledgements

Firstly, I would like to thank my parents Mr. Mahadeo Mali and Mrs. Chaya Mali for their constant love and support. I would like to thank them for believing in me, encouraging me throughout my schooling and my master's study. I would like to express my sincere gratitude to Prof. Dr. Subrata Sengupta with whom discussions about every aspect of engineering have proven to be of utmost importance in my work. I would like to thank him for providing me with the opportunity to work on Latent Heat Thermal Energy Storage Systems and their Optimization.

I would like express gratitude towards Prof. Dr. Oleg Zikanov, who helped me understand the concepts in Computational Fluid Dynamics in his ME 525 course and for being a part of my thesis committee. I would also like to thank Prof. Dr. Armen Zakarian for allowing me to study Design of Experiments course offered by Industrial and Manufacturing Systems Engineering department, and for being a part of my Master's thesis committee.

I would also like to thank Suvil Kundapur, an UM-Dearborn alum and research colleague, who helped me in validating my computational results through experiments performed in the laboratory at UM-Dearborn. I would like to thank my fellow UM-Dearborn graduate students Akshaykumar Sakhare, Abhishek Mangoli, Suparshwa Keerthi for supporting me in my work with productive discussions and valuable suggestions.

Table of Contents

Acknowledgements.....	ii
List of Figures.....	v
List of Tables.....	vi
Abstract.....	vii
Chapter 1 Introduction.....	1
1.1 Introduction to Thermal Storage.....	1
1.2 Background and Motivation.....	1
1.3 Problem Definition.....	2
1.4 Literature Review.....	2
Chapter 2 Numerical Modelling and Validation.....	5
2.1 System Description.....	5
2.2 CFD Modelling.....	6
2.2.1 Geometry.....	6
2.2.2 Mesh.....	7
2.2.3 CFD Setup and Solution.....	8
2.2.4 Post Processing:.....	13
2.2.5 Parameterization of Variables.....	13
2.2.6 Discussion of melting of PCM inside a cylinder.....	14
Chapter 3 Response Surface Modelling and Genetic Algorithm.....	16
3.1 Theory.....	16
3.2 Selection of Response Surface Designs.....	17
3.3 CCD for current work.....	18
Chapter 4. Optimization.....	23
4.1 Optimization theory.....	23
4.2 Genetic Algorithm.....	24
4.3 Single Objective Optimization.....	25
4.3.1 Initial population (design points).....	25
4.3.2 Selection.....	25

4.3.3 Generating new population.....	25
4.3.4 Crossover	26
4.3.5 Mutation.....	26
4.4 Multi-objective optimization.....	27
4.4.1 Pareto dominance	27
Chapter 5 Results	29
5.1 Case 1: Optimization of Weight (Unconstrained).....	29
5.2 Case 2: Optimization of Melt time (Unconstrained).....	30
5.3 Case 3: Multi objective optimization of Weight vs Melt time without constraint.....	31
5.4 Case 4: Optimization of Weight (Heat Capacity as constraint)	33
5.5 Case 5: Optimization of Melt time (Heat Capacity as constraint)	35
5.6 Case 6: Multi objective optimization of Weight vs Melt time (Heat Capacity constraint). 35	
Chapter 6 Conclusion.....	41
6.1 Future scope	41
Appendix Software Interfaces.....	43
References.....	51

List of Figures

Figure 1 Schematic drawing of the Problem Setup	2
Figure 2 Experimental Setup (Actual photo)	6
Figure 3 Geometry (CAD model) for the CFD Modelling	7
Figure 4 Mesh for the Experimental Setup (Complete Geometry)	8
Figure 5 Mesh for Experimental Setup (Zoomed - in)	8
Figure 6 Velocity vector CFD result for the experimental setup	15
Figure 7 Melt fraction CFD results for experimental setup	15
Figure 8 Response Surface for CFD Melt time	20
Figure 9 Response Surface for Weight of Capsule	21
Figure 10 Goodness of fit for Melt time	22
Figure 11 Weight vs Melt time Pareto front - Case 1	30
Figure 12 Weight vs Melt time Pareto front - Case 2	31
Figure 13 Weight vs Melt time Pareto front - Case 3	32
Figure 14 Weight vs Melt Time Optimal Pareto chart - Case 3	33
Figure 15 History of Convergence of Heat Capacity - Case 4	34
Figure 16 Weight vs Melt time Pareto Plot – Case 4	34
Figure 17 Weight vs Melt time Pareto plot - Case 5	35
Figure 18 Weight vs Melt time Optimal Pareto Chart - Case 6	36
Figure 19 Weight vs Melt Time Global Optimal Pareto Chart	36
Figure 20 Weight vs Melt time Pareto front progression	37
Figure 21 History of Convergence of Heat Capacity - Case 6	38
Figure 22 History of Convergence of Weight	38
Figure 23 History of Convergence of Melt time - Case 6	39
Figure 24 History of Convergence of OD	39
Figure 25 History of Convergence of Wall Thickness - Case 6	40
Figure 26 ANSYS Workbench Project Layout	43
Figure 27 ANSYS Design Modeler Interface	44
Figure 28 ANSYS Mesher Interface	45
Figure 29 ANSYS FLUENT Interface	46
Figure 30 Input and Output Parameter Set	47
Figure 31 ANSYS Design of Experiments Interface	48
Figure 32 ANSYS Response Surface Interface	49
Figure 33 ANSYS Optimization Interface	50

List of Tables

Table 1 PCM Properties.....	5
Table 2 Experimental Setup Details	6
Table 3 CFD Solver setup.....	11
Table 4 Comparison between CFD and Experimental results	13
Table 5 Design of Experiments details	19
Table 6 Central Composite Design Points with grid details	19
Table 7 Central Composite Design Points Results	20
Table 8 Optimization algorithm details (ANSYS Design Explorer)	28
Table 9 Results Case 1	30
Table 10 Results - Case 2.....	31
Table 11 Results - Case 4.....	34
Table 12 Results - Case 5.....	35

Abstract

Product development processes involve computational methods like Computational Fluid Dynamics to simulate real world fluid flow and heat transfer phenomena numerically using computers. Also, traditional heuristic design methods require enormous numerical simulations to obtain optimum designs which makes these methods inefficient and highly expensive. This thesis presents a design of experiments - based approach to develop an optimization tool that can predict the optimum performance of a Thermal Energy Storage (TES) system using Computational Fluid Dynamics (CFD) [1], Response Surface Methodology (RSM) [2] [3], and Genetic Algorithm [4]. A cylindrical capsule filled with Phase Change Material (PCM) is used as a Thermal Energy Storage (TES) system or Latent Heat Thermal Energy Storage (LHTES) system, which stores and releases heat as the PCM melts or solidifies respectively. Based of literature review and previous research, Outer Diameter and Wall thickness of the capsule were considered as the possible influencing parameters (i.e. design variables), whereas Melt time of PCM and Weight of cylindrical capsule were considered as the objective functions (output responses). The effects of design variables on the objective functions was studied using the results of CFD simulations and Central Composite Design as the Design of Experiments type. Single and Multi-Objective optimization was performed to find best possible results for the above two objectives in 6 different cases. A robust optimization tool for a thermal battery design was developed which in theory could be applied to any type of heat exchanger design to reduce the overall product development time.

Chapter 1 Introduction

1.1 Introduction to Thermal Storage

Latent Heat Thermal Energy Storage Systems (LHTES) based on Phase Change Materials (PCMs) have been a part of research for many years [5] [6]. LHTES technology makes use of the sensible heat of a Heat Transfer Fluid (HTF) for melting and solidification of the PCM to store and release energy. Applications of such systems range from space heating and cooling, solar energy applications, heating, ventilation and air conditioning in buildings, electrified vehicles to peak load reduction [6].

Design of LHTES systems involves selection of geometric parameters and operating conditions that provide for maximum heat transfer with a minimum pressure drop. Numerical modelling and CFD correlated with experimental results have been traditionally used for the development of these systems. But these methods demand substantial amount of resources to provide an optimized design. An optimization tool that takes design variables (like geometric parameters) as input and gives an optimized design as output efficiently, would yield considerable economic advantages.

1.2 Background and Motivation

Design of a mechanical system involves selection from multiple levels of parameters. The performance of and mechanical system based on one set (or combination) of parameters (or design variables) was traditionally evaluated using experiments by building prototypes. Due to later developments in the field of Computational Methods, the need for building prototypes was reduced. These evaluations could be done using Computational Fluid Dynamics (CFD). The procedure for CFD includes Pre-processing (building a Computer-Aided-Design (CAD) model, grid generation, setting up the solver parameters), processing (solving) and post-processing. The problem with this method is each time the set of parameters change; a new model is needed to be analyzed. Thus, coming up with an optimized design demands enormous computing power and

consequently time, money, and labor. Therefore, there is a need to develop an algorithm to provide optimized design for a multitude of design variables.

1.3 Problem Definition

The Latent Heat Thermal Energy Storage (LHTES) system under consideration in this work is a cylindrical capsule filled with a phase change material (PCM) at room temperature (25 deg C). Hot air at 70 deg C is passed over the cylinder placed horizontally. Fig. 1 shows a schematic of the experimental setup. Due to a temperature difference between the air and the cylindrical capsule, there will be heat transferred to the PCM and it will melt over time. Thus, the PCM stores energy as it heats and melts. Designing of this system, involves selection of geometric parameters like Outer diameter (OD) of the tube, Wall thickness (WT) of the tube. In a heuristic design approach, an iterative method is performed in which the designer guides the design process based on the results of the previous iteration. But this method is expensive and exhausting. This work aims to develop a more efficient way than a heuristic approach to find geometric dimensions of the cylindrical capsule that yield optimum *Weight of capsule* and *Melt time* of PCM.

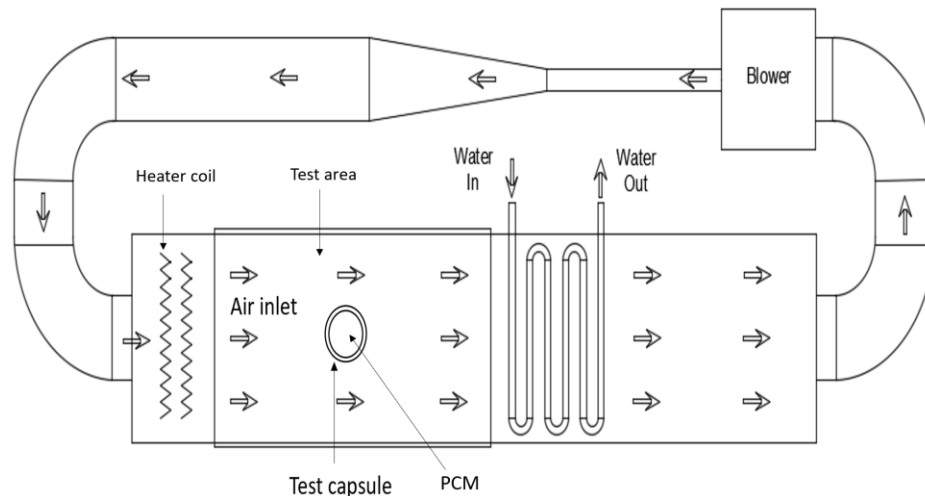


Figure 1 Schematic drawing of the Problem Setup

1.4 Literature Review

Latent heat as a medium for thermal energy storage has been a part of academic and industry research for several years. Z. Ling et. al. has researched latent heat thermal energy storage systems that are used for thermal management of electronic systems [5]. Ioan Sarbu et. al. focussed on TES

technologies that provide a way of valorizing solar heat and reducing the energy demand on buildings [6].

Computational Fluid Dynamics (CFD) and numerical solution techniques have been extensively used to analyze the heat transfer and melting phenomena in such systems for quite some time. Beer and Bareis provided a closed form solution of the melting process inside a horizontal tube, which was validated by their experiments using a photographic technique. N-octadecane and p-xylene were used as the PCM for their work [7]. Melting rates and heat transfer co-efficients were in good agreement with the experiment. A Atal et. al. used ANSYS Fluent CFD to study the effects of metal foam on melting of Phase Change Material in horizontal shell and tube exchanger [8].

Maldonado investigated the melting process inside a horizontal cylinder as part of his Masters thesis at University Miami [9]. Octadecane was used as the PCM. Ajay Prasad investigated the effects of natural convection on the melting inside a horizontal cylinder as part of his Masters thesis at University of Miami [10]. Both, Prasad's and Maldonado's work played a major part and influenced the planning and execution of the experiments performed in the current work.

These LHTES systems can be designed in various size and configurations. CFD has a high potential to easily explore a large number of different configurations. However, due to enormous computing times required for these CFD simulations; design exploration, what-if studies and optimization is rendered impractical. Response Surface Methodology (RSM) has been increasingly used for optimization problems involving CFD. Krajnovic studied aerodynamic optimization of vehicles using CFD and RSM [11]. This study involved 4 design variables and 2 objective functions. Face Centered Composite Design was used as the DoE technique to build a 2nd order polynomial RS. Optimization method used was e-constrained method. Hierarchical cluster algorithm was used to analyze the Pareto Optimal solutions.

Lohrasbi et al. used Response Surface Method along with Finite Element Analysis to optimize a novel fin-array for multiple objectives [3]. Considering maximum heat storage capacity, the optimization procedure led to efficient shape design of the LHTES system. A Sciacovelli et al. enhanced the performance of a shell-tube LHTES unit by optimizing the geometry of Y-shaped fins through the combined use of CFD and RSM [12]. 30 design points were used to build the Response Surface model which was later used for optimization studies.

Hedderich et. al. used the method of feasible directions and Augmented Lagrange multiplier method for the design and optimization of air-cooled tube bank heat exchangers [13]. However, Classical Optimization techniques like method of feasible directions, are known for their lack of robustness and for their tendency to fall into local optima.

Researchers have been exploring other non-gradient based optimization algorithms in recent years. Asadi et. al. used a cuckoo search algorithm for the economic optimization of shell and tube heat exchangers [14]. Methods like Evolutionary Algorithms (EAs) offer several attractive features and have been widely used for design shape optimization, moreover for multi-objective multi parameter problems [4].

Dominique Thevenin et al studied optimization of a cross-flow tube bank heat exchanger [15]. The problem was to optimize the positions of tubes using Evolutionary Algorithms (EAs) so that the heat exchange is maximal while keeping a minimal pressure loss. Godarzi et. al. optimized a PCM storage system for a solar absorption chiller using genetic algorithm [16]. R. Raud et al. presented an analytical method for optimizing the design of a tube and shell type heat exchanger subject to geometric and performance constraints [17]. Their optimization method was used to investigate the relationship between optimal vessel geometry and configuration, fin properties, PCM properties, and the cost of two PCMs.

As a whole, optimization of configurations involving coupled CFD simulation of flow and heat transfer remains a fairly new field of research. And, the use of such optimization methods for design of LHTES systems involving cylindrical capsules is limited. This work aims at providing an in-depth understanding of the genetic algorithm optimization method as applied to the melting process of a PCM in a horizontal cylindrical capsule.

Chapter 2 Numerical Modelling and Validation

2.1 System Description

Thermal energy is stored in the form of latent and sensible heat in the Phase Change Material (PCM) which is contained in a cylindrical capsule. The PCM used for this study is A58h from the company PCM Products Ltd. The physical and thermal properties of the PCM are described in table 1. PCM is filled in a cylindrical capsule which is made of 6061 Aluminum. The outer diameter of the capsule is 0.5 inch with a 1.25 mm wall thickness. This capsule is sealed from both ends to prevent leaking of the melted PCM. This cylindrical capsule is placed in a crossflow of hot air in a wind tunnel. Inlet temperature of the air is 70 deg C, and an inlet velocity of 2.33 m/s averaged over the length of the cylinder is used for melting the PCM in the cylindrical capsule. The experimental setup details are shown in table 2. Fig. 2 shows the arrangement of the cylindrical capsule placed in crossflow. Photographic observations of the melting phenomena were made to validate the CFD results. Experimental melt time of the PCM is defined as the time taken by the PCM from the start of melting of the outer most layer of PCM inside the tube to the complete melting of the PCM in the tube as observed in the experiment.

Table 1 PCM Properties

PCM	A58h	Units
Type	Organic A	
Phase Change Temperature	58	deg C
Density	820	kg/m ³
Latent Heat Capacity	243	kJ/kg
Volumetric Heat Capacity	199	MJ/m ³
Specific Heat Capacity	2.85	kJ/kg-K
Thermal Conductivity	0.18	W/m-K
Max. Operating Temperature	300	deg C

Table 2 Experimental Setup Details

<i>Dimensions</i>	
Outer diameter of the capsule (OD)	12.7 mm
Wall thickness of the capsule (WT)	1.25 mm
<i>Operating conditions</i>	
Inlet velocity	2.33 m/s
Inlet Temperature	70 deg C



Figure 2 Experimental Setup (Actual photo)

The optimization problem using CFD analysis requires CFD simulations/experiments for a number of design points. The following section will describe the sample CFD Modelling for the given set of the input and output parameters in the experimental setup.

2.2 CFD Modelling

The system described in the experiment is modeled using ANSYS Workbench for CFD analysis.

2.2.1 Geometry

Fig. 3 shows the geometry used for the CFD Analysis created using ANSYS DesignModeler. Since the cylindrical capsule was placed horizontally in crossflow of air, and assuming that the cylinder is a long cylinder, there is a fairly negligible change in the velocity profile along the length of the cylinder. Thus, the problem can be reduced to a 2D heat transfer and fluid flow analysis. Also, since the assumption of a 2D flow is sufficiently accurate, the time and computing power required

for the 2D CFD simulations is greatly reduced compared to a 3D problem. The air domain is considered to be sufficiently large such that it does not affect the flow around the cylinder.

The outer diameter and the wall thickness of the capsule are parameterized in ANSYS Design Modeler for design exploration [18]. Geometric dimensions for all the subsequent DoE design points used to generate a response surface approximation are mentioned in the table.

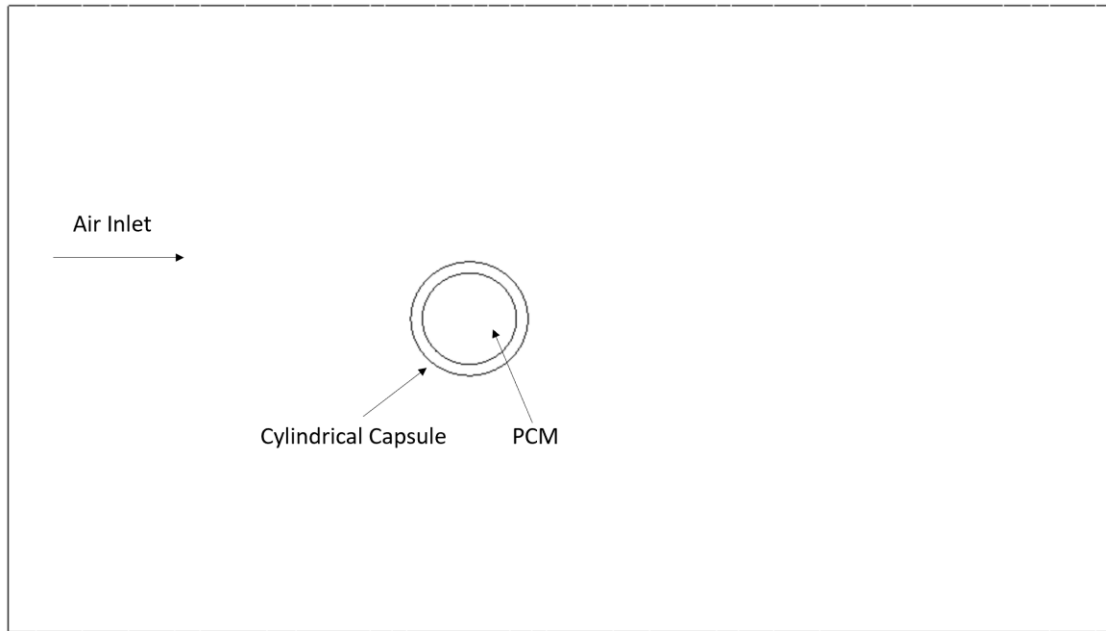


Figure 3 Geometry (CAD model) for the CFD Modelling

2.2.2 Mesh

The geometry created in Design Modeler was discretized using ANSYS Mesher. Considering the PCM and Air are modeled as fluid domains and the capsule is considered to be a solid domain, variable grid sizes were used in this model. Since the outer wall of the cylinder is considered to be a no-slip boundary, there will be a boundary layer generated around the cylinder wall [19]. Thus, the grid needs to be fine to resolve the velocity gradients accurately. After performing a grid sensitivity study, grid sizes of 1 mm, 0.5 mm, 0.4 mm were used for Air, PCM and capsule respectively. Fig. 4 and fig. 5 show the grid for current geometry described in the above experimental setup which consisted of 12721 elements.

The grid for all the DoE points used for Response Surface modelling were generated individually and details are mentioned in table.

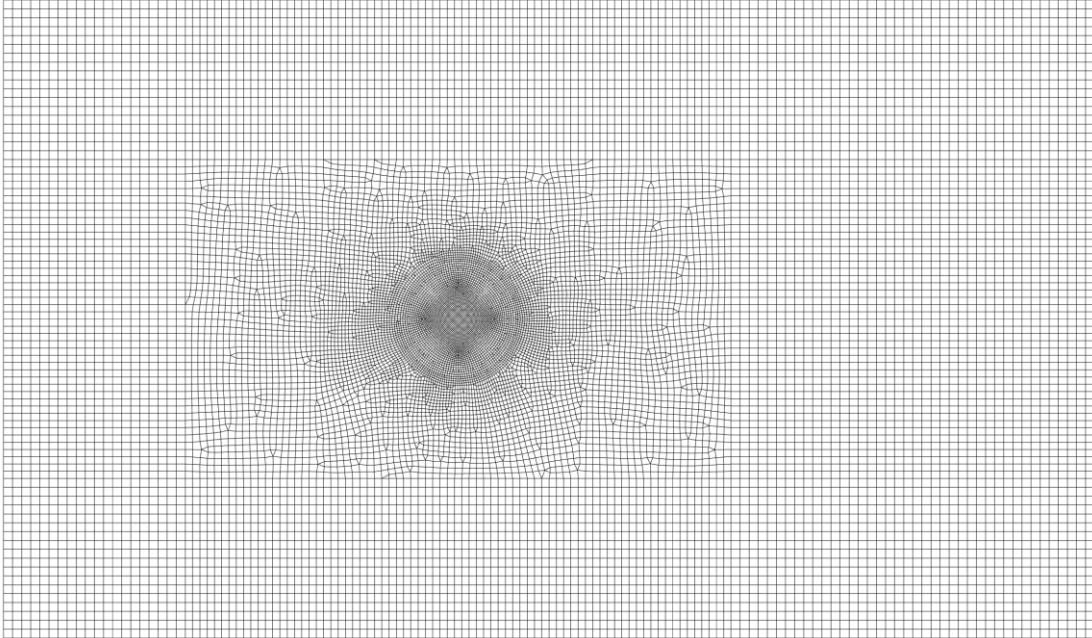


Figure 4 Mesh for the Experimental Setup (Complete Geometry)

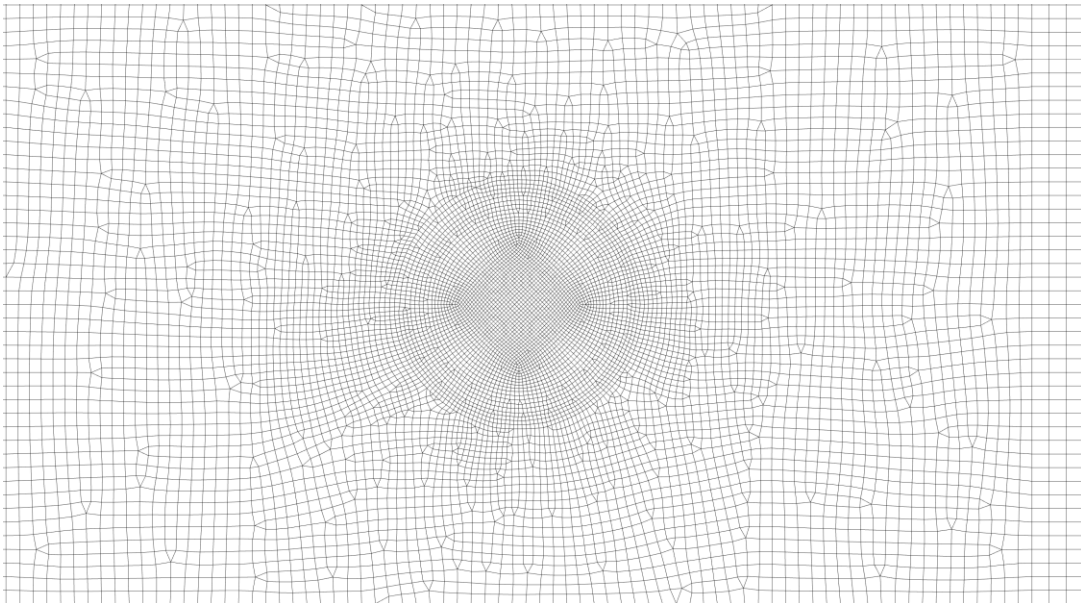


Figure 5 Mesh for Experimental Setup (Zoomed - in)

2.2.3 CFD Setup and Solution

The numerical simulation for the grid generated using ANSYS Mesher is solved in ANSYS Fluent module. The Reynolds number for this flow is calculated to be 1484 [20] using the following equation,

$$Re \# = \frac{U_{avg} * D}{\nu}$$

where, U_{avg} = average velocity of inlet air

D = characteristic length of flow i.e. Diameter of capsule

$$\nu = 1.79 \frac{m^2}{s}$$

Thus, the flow is modeled as a laminar unsteady flow. Solidification & Melting model is used to simulate the melting process of the PCM. A numerical solution for this setup was obtained by solving the following equations:

Governing equations:

ANSYS FLUENT solves the following equations for mass and momentum [18].

The equation for conservation of mass, or continuity equation is given by,

$$\frac{\partial \rho}{\partial t} + \nabla \cdot (\rho \vec{v}) = 0$$

Conservation of momentum in an inertial (non-accelerating) reference frame is given by,

$$\frac{\partial}{\partial t} (\rho \vec{v}) + \nabla \cdot (\rho \vec{v} \vec{v}) = -\nabla p + \nabla \cdot (\bar{\tau}) + \rho \vec{g} + \vec{F}$$

where p is the static pressure, $\bar{\tau}$ is the stress tensor (described below), and $\rho \vec{g}$ and \vec{F} are the gravitational body force and external body forces (e.g., that arise from interaction with the dispersed phase), respectively. \vec{F} also contains other model-dependent source terms such as porous-media and user-defined sources.

General equation for stress tensor is $\bar{\tau}$ is given by,

$$\bar{\tau} = \mu \left[(\nabla \vec{v} + \nabla \vec{v}^T) - \frac{2}{3} \nabla \cdot \vec{v} I \right]$$

where μ is the molecular viscosity, I is the unit tensor, and the second term on the right-hand side is the effect of volume dilation. This equation is modified accordingly for incompressible fluids.

ANSYS FLUENT solves the energy equation in the following form:

$$\frac{\partial}{\partial t}(\rho E) + \nabla \cdot (\vec{v}(\rho E + p)) = \nabla \cdot \left(k_{eff} \nabla T - \sum_j h_j \vec{J}_j + (\bar{\tau}_{eff} \cdot \vec{v}) \right) + S_h$$

where k_{eff} is the effective conductivity ($k + k_t$, where k_t is the turbulent thermal conductivity, defined according to the turbulence model being used), and \vec{J}_j is the diffusion flux of species j . The first three terms on the right-hand side of above equation represent energy transfer due to conduction, species diffusion, and viscous dissipation, respectively. S_h includes the heat of chemical reaction, and any other volumetric heat sources you have defined.

ANSYS FLUENT uses an enthalpy porosity formulation [21] [22], for solving solidification and melting problems. The enthalpy of the material is computed as the sum of the sensible enthalpy, h , and the latent heat, ΔH :

Where

$$H = h + \Delta H$$

$$h = h_{ref} + \int_{T_{ref}}^T c_p dT$$

$$h_{ref} = \text{reference enthalpy}$$

$$T_{ref} = \text{reference temperature}$$

$$c_p = \text{specific heat at constant pressure}$$

The liquid fraction, β , can be defined as

$$\beta = 0 \text{ if } T < T_{solidus}$$

$$\beta = 1 \text{ if } T > T_{solidus}$$

$$\beta = \frac{T - T_{solidus}}{T_{liquidus} - T_{solidus}} \text{ if } T_{solidus} < T < T_{liquidus}$$

The latent heat content can now be written in terms of the latent heat of the material, L :

$$\Delta H = \beta L$$

The latent heat content can vary between zero (for a solid) and L (for a liquid).

For solidification/melting problems, the energy equation is written as

$$\frac{\partial}{\partial t}(\rho H) + \nabla \cdot (\rho \vec{v} H) = \nabla \cdot (k \nabla T) + S$$

where, $H = \text{enthalpy}$

$\rho = \text{density}$

$\vec{v} = \text{fluid velocity}$

$S = \text{source term}$

The solution for temperature is essentially an iteration between the energy equation and the liquid fraction equation. Directly using equation for energy to update the liquid fraction usually results in poor convergence of the energy equation. In **ANSYS FLUENT**, the method suggested by Voller and Swaminathan [23] is used to update the liquid fraction. For pure metals, where $T_{solidus}$ and $T_{liquidus}$ are equal, a method based on specific heat, given by Voller and Prakash [22], is used instead.

The solver setup details are mentioned in the table 3. The solution is initialized using the default values in ANSYS Fluent. A time convergence study was conducted which yielded 0.05 s to be the best compromise between an accurate solution and the total time required for the simulation. The total flow time of the analysis was chosen to be equal to that required for real time melting of the PCM observed in the experiment. Simulation data was saved at every 15 seconds of flow time. The CFD solver setup described in table. 3 was maintained constant throughout all the DoE points used for Response Surface Modelling.

Table 3 CFD Solver setup

<u>Solver</u>	
Type	Pressure – based
Time	Transient
2D space	Planar
Velocity formulation	Absolute
<u>Models</u>	

Energy	
Solidification and Melting	
Viscous	Laminar
<u>Solution Methods</u>	
Pressure - Velocity Coupling	
Scheme	SIMPLE
<u>Spatial Discretization</u>	
Gradient	Least squares cell based
Pressure	Second Order
Momentum	Second Order Upwind
Energy	Second Order Upwind
Transient Formulation	First Order Implicit
<u>Solution Controls</u>	
Under-Relaxation Factors	
Pressure	0.3
Density	1
Body Forces	1
Momentum	0.7
Liquid Fraction Update	0.9
Energy	1
<u>Residuals Criteria</u>	
Continuity	0.001
x-velocity	0.001
y-velocity	0.001
energy	1E-06
Scaled	Yes
<u>Time Step</u>	
Time step size	0.05 s
Number of Time steps	30000
Max Iterations/Time Step	20

2.2.4 Post Processing:

The results of the CFD analysis were observed in ANSYS CFD Post. Fig. 7 shows melting of a PCM inside a horizontal cylindrical capsule placed in a crossflow over a period of time. Fig. 6 shows the velocity vectors for the current setup at the end of the simulation. Table 4 shows a comparison between the experimental and CFD Melt times and it was observed that the CFD results were in enough agreement with the experiments considering the melting and solidification model used in this analysis.

The Melt fraction contours were used to calculate time required for the melting of the PCM. *CFD melt time* is defined as the time measured from start of melting of outermost layer of the PCM, to end of melting of the all the PCM contained in the capsule. This *CFD melt time* was used as a performance metric for all the DoE design points. The aim of the optimization study is to minimize the *CFD melt time*.

Weight of the capsule is defined as the total weight of the PCM contained in the cylindrical capsule plus the weight of the cylindrical capsule. This weight is used a performance metric for all the DoE design points. The aim of the optimization study is to minimize the *weight of the capsule*.

Table 4 Comparison between CFD and Experimental results

Outer Diameter (mm)	Wall thickness (mm)	CFD Melt time	Experimental Melt time
12.7 mm	1.25 mm	1290 s	907 s

2.2.5 Parameterization of Variables

Design Parameters like Outer Diameter and Wall thickness of capsule and Output Responses like Melt time will be used as Input Parameters for generating Design of Experiments. There is a need to parameterize these quantities so that they can be updated at a project level (from ANSYS Workbench). This is done by setting the OD and Wall thickness as parameters in Design Modeler interface. Melt time is calculated by visually observing the melt fraction of PCM over time in CFD Post. Weight and Heat Capacity of capsule is calculated as follows:

1. *Inner Diameter of Capsule* = $OD - 2 * Wall\ thickness$
2. *Volume of PCM in capsule* = $\frac{\pi}{4} * ID^2 * L$
3. *Volume of Rod* = $\frac{\pi}{4} * (OD^2 - ID^2) * L$

4. *Volume of Capsule = Volume of PCM + Volume Rod*
5. *Mass of PCM = ρ_{PCM} * Volume of PCM*
6. *Mass of Rod = ρ_{Al} * Volume of Rod*
7. *Sensible Heat of PCM = Mass of PCM * Sp.Heat of PCM * (70 – 27)*
8. *Sensible Heat of Rod = Mass of Rod * Sp.Heat of Rod * (70 – 27)*
9. *Latent Heat of PCM = Mass of PCM * Latent Heat Capacity of PCM*
10. *Weight = Mass of PCM + Mass of Rod*
11. *Heat Capacity = Sensible Heat of PCM + Sensible Heat of Rod +
Latent Heat of PCM*

where, OD – Outer Diameter of Capsule

ID – Inner Diameter of Capsule

L – Length of cylinder

ρ_{PCM}, ρ_{Al} – Mass Densities of PCM and Capsule Material respectively

2.2.6 Discussion of melting of PCM inside a cylinder

As hot air flows over the cylindrical capsule, solid PCM starts melting due to heat transfer between the air (HTF) and PCM. The outside layer of PCM melts rapidly due to higher temperature gradient between air and PCM. But the melting gradually slows down as heat transfer rate reduces due to decreasing temperature gradients. In the current CFD setup, gravitational acceleration is not considered. Thus, although in reality, sinking of solid PCM in the cylinder is seen, we do not observe the same in the current results. Also, because of sinking of PCM, the ideal way to model the melting phenomena would be to consider the solid PCM as a hydrodynamic journal bearing, whose weight is supported by the pressure generated in the layer of liquid PCM between solid PCM and metal capsule. However, results obtained using simplified modelling of the current setup are satisfactory for the current scope of the project. This type of modeling does give us appreciable insight into melting process of the PCM inside a horizontal cylindrical capsule.

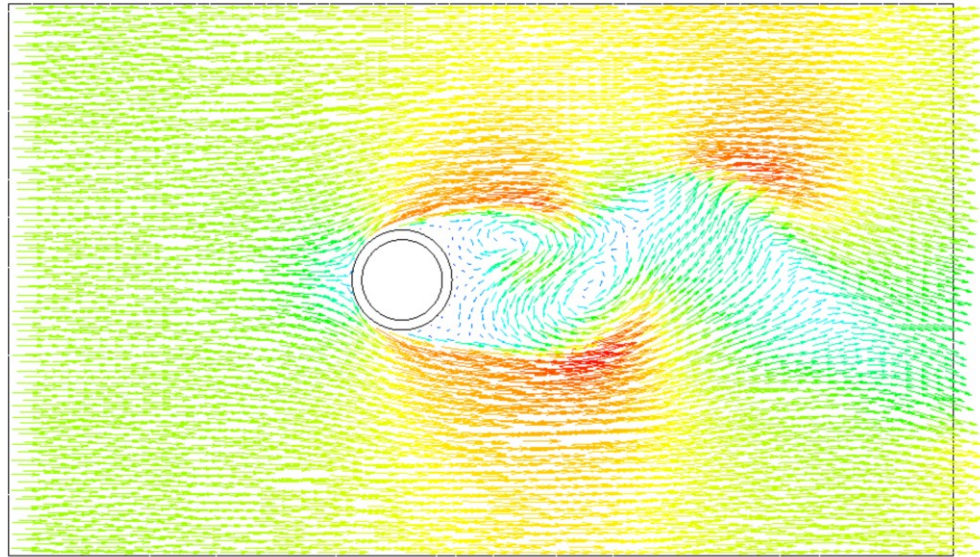
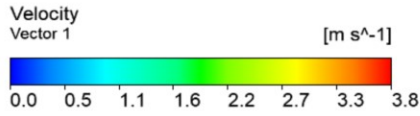


Figure 6 Velocity vector CFD result for the experimental setup

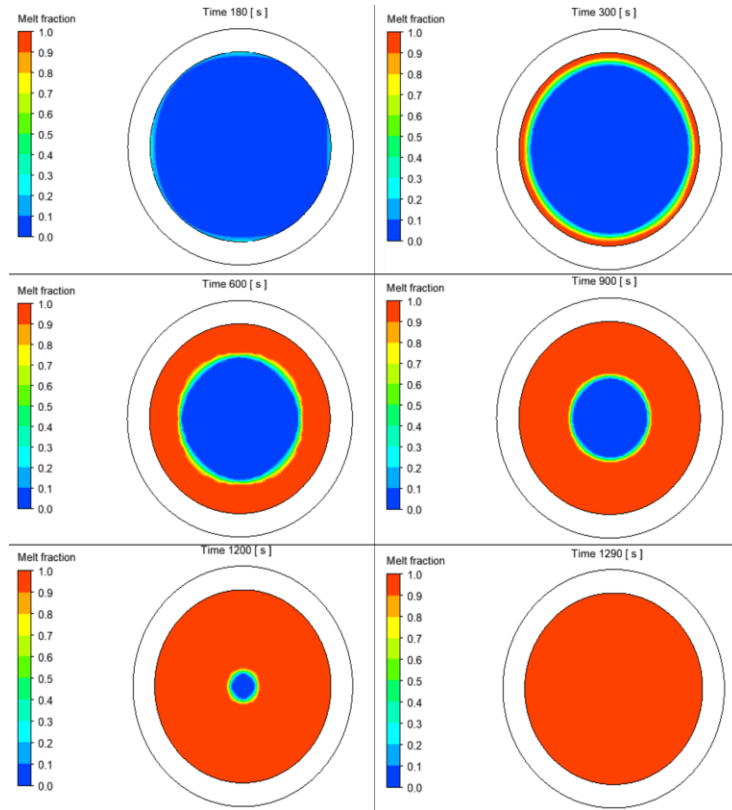


Figure 7 Melt fraction CFD results for experimental setup

Chapter 3 Response Surface Modelling and Genetic Algorithm

3.1 Theory

Response Surface Modelling is a collection of mathematical and statistical techniques useful for the modelling and analysis of problems in which a response of interest is influenced by several variables and the objective is to optimize this response [24].

In most RSM problems, the form of the relationship between the response and the independent variables is unknown. Thus, the first step in RSM is to find a *suitable approximation* for the true functional relationship between the response and set of independent variables.

If the response is well modelled by a linear function of the independent variables, then the approximating function is the *first order model*

$$y = \beta_0 + \beta_1 x_1 + \beta_2 x_2 + \cdots + \beta_k x_k + \epsilon$$

If there is a curvature in the system, then a polynomial of higher degree must be used, such as the *second order model*,

$$y = \beta_0 + \sum_{i=1}^k \beta_{1i} x_i + \sum_{i=1}^k \beta_{2i} x_i^2 + \sum_{i < j} \beta_{ij} x_i x_j + \epsilon$$

The method of least squares is used to estimate the parameters in the approximating polynomials [21].

This fitted response surface is then used for optimizing the input variables versus output responses. If the fitted response surface is an adequate approximation of the response function, then analysis of the fitted surface will be approximately equivalent to the analysis of the actual system. A response surface is approximated for each output response.

Coefficient of determination (R^2) is used to analyze the goodness of fit for each response surface. Coefficient of determination is the percent of the variation of the output parameter that can be explained by the response surface model. That is, the Coefficient of Determination is the ratio of the explained variation to the total variation. The best value is 1 [18].

Mathematically represented as:

$$1 - \frac{\sum_{i=1}^N (y_i - \hat{y}_i)^2}{\sum_{i=1}^N (y_i - \bar{y}_i)^2}$$

The model coefficients (weights) from the first or second order models can be estimated most effectively if proper experimental/simulation designs are used to collect data. Designs for fitting response surface are called *response surface designs*.

3.2 Selection of Response Surface Designs

Design of Experiments (DoE) is used to generate the set of design points needed to collect the data set for building the response surface models. Among the different types of DoE techniques available in the literature, a few of them are listed below: -

1. Full factorial designs
2. Fractional factorial designs
3. Central Composite Design
4. Box - Behnken Design
5. D-Optimal design
6. Taguchi Design [25]

Following characteristics are needed to be considered while choosing a DoE method [24]:

The DoE method should,

1. provide a reasonable distribution of data points throughout the region of interest
2. provide precise estimates of the model co-efficients
3. provide reasonable robustness against outliers or missing values

4. not require a large number of runs
5. not require too many levels of the design variables

Central Composite design (CCD) is often used for optimization problems within the framework of CFD applications [26]. CCD is a very efficient design for fitting the second order polynomial approximations.

There are three types of design points in a CCD [24]

1. two-level factorial/fractional factorial designs (2^{k-f}) which builds a basic linear approximation model between the design variables and output responses,
2. $2 * k$ axial (star) points at a distance α , to estimate curvature in the relationship,
3. n center points, which provide a good and independent estimate of the experimental/simulation error

Thus, the total number of designs in a CCD will be,

$$N = 2^{k-f} + 2 * k + n$$

α is an important parameter used in CCD to decide the location of the design points within the design space. Its value is typically set to be $\alpha = (n_f)^{\frac{1}{4}}$ or $\alpha = \sqrt{k}$ or 1.

3.3 CCD for current work

The input parameters 1) *Outer Diameter (OD)*, and 2) *Wall thickness of the tube (WT)*, are considered as the design variables. 1) *CFD Melt time* of the PCM as defined in the CFD Modelling in the previous chapter and 2) *Weight of the cylindrical capsule*, are considered as the output responses.

ANSYS Design Exploration system within ANSYS Workbench software, was used to generate the Central Composite Designs. For 2 input parameters, 9 design points are required to build a response surface using the CCD [18]. $\alpha = 1$, is chosen to a suitable value for this analysis. The levels of factors used in this analysis are given in table 5. These levels are chosen based on the value of α . Thus, the CCD design becomes a face-centered composite design with the design points

as shown in the fig. The DOE matrix along with the grid sizes for all design points is shown in the table 6.

Table 5 Design of Experiments details

<u>DOE Type</u>	Central Composite Design					
Input Parameters	Type	<u>Design Space (Range)</u>		<u>Levels</u>		
		Lower Bound	Upper Bound			
OD (mm)	Continuous	6 mm	25.4 mm	6 mm	15.7 mm	25.4 mm
Wall Thickness (mm)	Continuous	0.5 mm	1.5 mm	0.5 mm	1 mm	1.5 mm

Table 6 Central Composite Design Points with grid details

<u>Input Parameters</u>			<u>Grid sizes (mm)</u>			
Design Point #	OD (mm)	Wall Thickness (mm)	PCM	Capsule	Air	# of elements
1	15.7	1	0.5	0.2	1	27283
2	6	1	0.6	0.3	0.8	18156
3	25.4	1	0.6	0.3	1	62414
4	15.7	0.5	0.5	0.15	1	29360
5	15.7	1.5	0.5	0.3	1	24345
6	6	0.5	0.2	0.15	0.8	20482
7	25.4	0.5	0.6	0.15	1	70384
8	6	1.5	0.2	0.3	0.8	18804
9	25.4	1.5	0.6	0.3	1	62421

9 design points given in the table were simulated using the CFD modelling technique mentioned in chapter 2. Each design point was simulated individually and output responses for the Melt time of the PCM and weight of the capsule were evaluated. Table 7 shows all input parameters with their corresponding output responses.

Table 7 Central Composite Design Points Results

OD (mm)	Wall Thickness (mm)	Melt time (s)	Weight (g)	Heat Capacity (KJ)
15.7	1	1875	33.21	8.18
6	1	210	7.14	1.26
25.4	1	4848	75.65	21.05
15.7	0.5	2080	27.52	8.00
15.7	1.5	1560	38.50	8.34
6	0.5	330	5.33	1.21
25.4	0.5	5191	66.07	20.75
6	1.5	130	8.54	1.31
25.4	1.5	4500	84.83	21.33

ANSYS Response Surface system used this dataset to build the initial Response Surface Model. Thus, a response surface was created for *CFD Melt time* and *Weight of the capsule* individually. Fig. 8 and fig. 9 shows the 3D response surface for the melt time and weight of the capsule. This Response surface can be used to predict the output responses for any combination of the design variables outside of the DoE points.

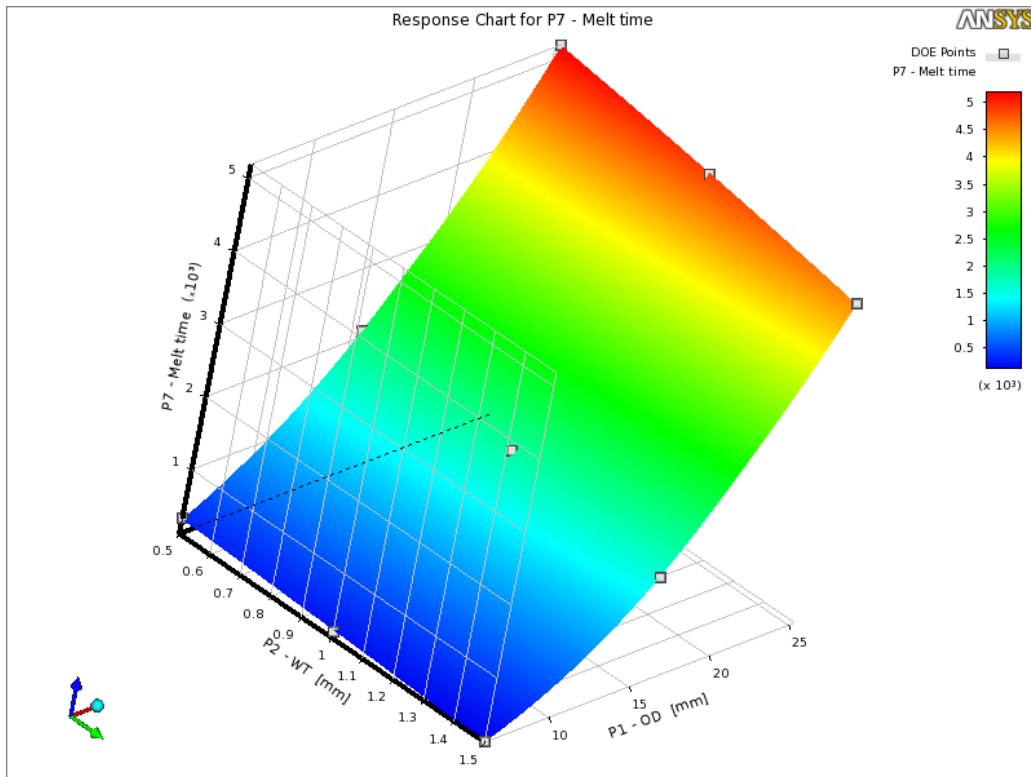


Figure 8 Response Surface for CFD Melt time

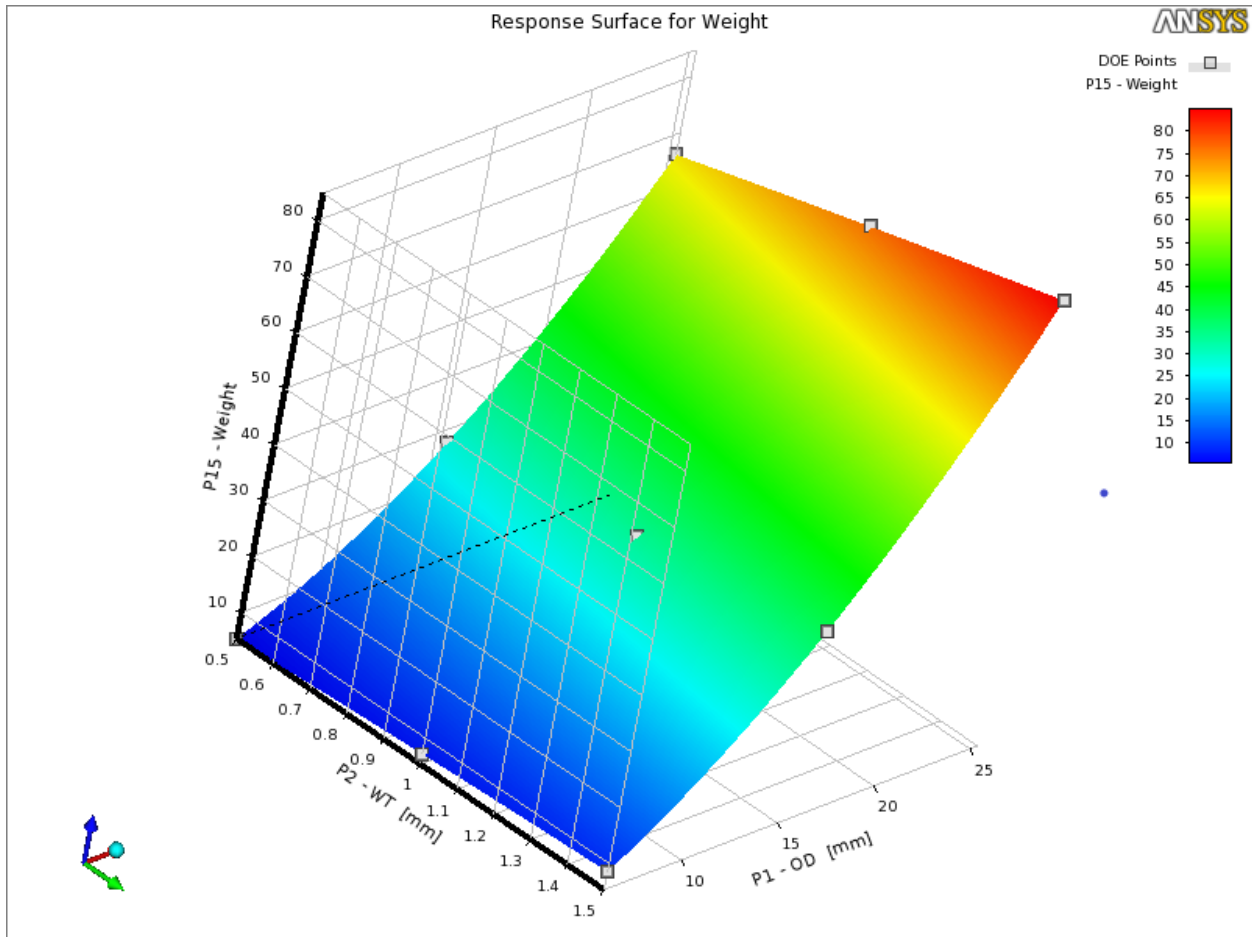


Figure 9 Response Surface for Weight of Capsule

Fig. 10 shows the predicted vs observed chart for *CFD Melt time*. This chart shows the output values for the 9 CCD design points predicted using the response surface vs the observed values using the CFD simulations. This chart is an indicator of the quality of the response surface and how well it fits the actual behavior between the input and output parameters (here outputs obtained using CFD are assumed to be their actual values). Any outliers in this chart will be an indication that the response surface is not accurately approximated in that region of the design space, and additional design points are needed in that region to improve the accuracy of the Response Surface Model.

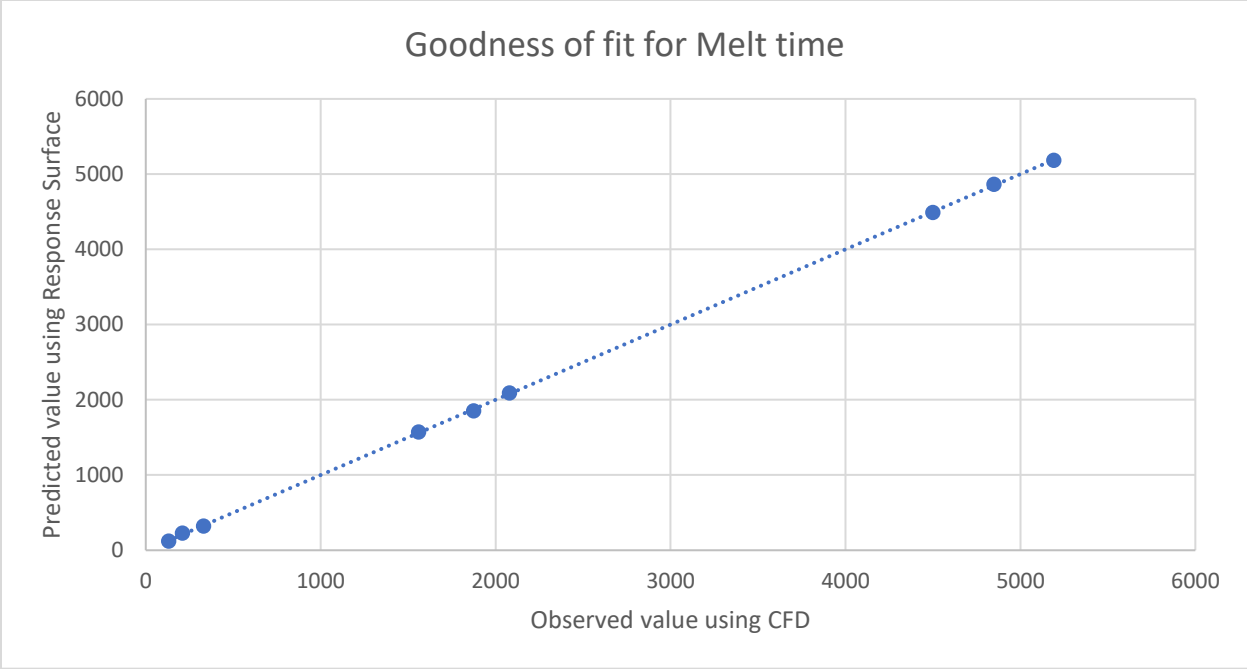


Figure 10 Goodness of fit for Melt time

Coefficient of determination of the initial Response Surface for melt time is given below for the initial Response Surface Model was found to be 0.99. Thus, it was concluded that this initial Response Surface approximation was sufficiently accurate to replace the CFD Analysis for further Optimization process.

Chapter 4. Optimization

4.1 Optimization theory

Optimization techniques as applied to engineering problems through numerical solutions give us an ordered approach to design decisions where before we relied heavily on intuition, experience and heuristic methods [27]. The purpose of numerical optimization is to aid us in rationally searching for the best design to meet our needs.

Various methods have been researched and used for optimization of problems involving use of CFD. Classical optimization methods such as Gradient Based Optimization [13], use a method of feasible directions. This optimization process can be thought of as climbing a hill with eyes blindfolded. Assuming one starts at the bottom of the hill, the goal is to reach the top of the hill. The approach here is to take finite steps in the direction of maximum gradient. Thus traditionally, the problem is defined as minimizing the negative of gradient of the hill. Gradient based Optimization is used by Vanderplaats for Marine Condenser Design [28].

The problem with this approach is that the method is very sensitive to the starting point of the optimization process. If there are local maxima in the vicinity of the starting point, GBO algorithms have a tendency to consider it as the final solution. Thus, finding a robust optimum design reliably, becomes a task of exhaustive search with multiple starting points.

Genetic Algorithm or Evolutionary Algorithms have proven to have a global perspective of the design space in finding optimal solutions and have been used for optimization of engineering problems for several years [4] [16]. The current work focusses on use of Genetic Algorithm (GA) for the optimization of *CFD melt time* and *Weight of the capsule* w.r.t. a horizontally placed cylindrical capsule placed in a crossflow.

Mathematically, an optimization problem is defined as [29],

$$\begin{aligned} & \text{Maximize or Minimize} && f_m(x), && m = 1, 2, \dots, M; \\ & \text{subject to} && g_j(x) \geq 0, && j = 1, 2, \dots, J; \\ & && h_k(x) = 0, && k = 1, 2, \dots, K; \\ & && x_i^{(L)} \leq x_i \leq x_i^{(U)}, && i = 1, 2, \dots, n. \end{aligned}$$

4.2 Genetic Algorithm

Evolutionary or Genetic Algorithms mimic evolutionary principles observed in nature such as natural selection, reproduction, crossover and mutation. The idea behind this method is that, an initial population of designs are generated within the design space by principles of crossover and mutation. These designs are then evaluated, and their output responses are used as performance metrics of each design. If the goal is to minimize an output response, the design with the least value of output will be ranked highest (strongest) in the population. Correspondingly, the design with the most value of the output will be ranked the lowest (weakest).

A selection procedure is used to eliminate weaker designs and reproduction will ensure parameters from the stronger designs are passed onto the next generation. This procedure of crossover, mutation, selection and reproduction is carried out over generations of populations till either the solution doesn't change anymore, or maximum number of generations have been evaluated. According to evolution theory, with every passing generation, a species becomes better at adapting to the surroundings. The reasoning is that, weaker entities within a generation are eliminated and traits from the stronger entities are passed onto the next generation which help the successive generations to become better at survival.

Thus, with every passing generation, it is expected that designs will approach the optimum values and the result would be a design that is better (meaning with maximum or minimum outputs depending upon the optimization objective) at the of the process.

4.3 Single Objective Optimization

4.3.1 Initial population (design points)

Number of Initial Design Points is decided by the user. This number must be greater than or equal to the sum of input and output parameters. Minimum recommended design points is 10 times the number of input parameters. Larger the initial set, better are the chances to find the input parameter space that contain the best solutions. The initial population (set of design points) is generated using Screening method (Shifted Hammersley Sampling) [18].

4.3.2 Selection

The principal idea behind selection is to guide the optimization process towards better designs within the design space. We ensure this by eliminating weak designs and giving more chances to the stronger designs to survive and reproduce in the optimization process. At the beginning of the selection process, we have N design points (either from the initial sampling in the 1st iteration or from previous iterations). Through selection we need to eliminate a finite number of design points that are weak as compared to other stronger design points. Strength of each design point is judged by its respective objective value. For example, in a minimization problem, design point having least objective value among the N design points will be the strongest and that having the largest objective value will be the weakest. The design points that clear the process of selection are passed on to crossover and mutation for reproduction to generate new design points. Tournament selection and ranking methods are most popular for single objective optimization in literature [29].

4.3.3 Generating new population

Once the weaker designs are eliminated using the selection procedure, the design space is explored using stronger design points and the method of crossover and mutation to find better solutions than the previous generation. According to the theory of evolution, these stronger design points from a previous generation will reproduce even stronger design points. Based on a) the number of design points per iteration (population) required, b) probability of crossover and probability of mutation, the division of number of points between selection, crossover, and mutation are decided by the algorithm.

4.3.4 Crossover

Crossover combines two designs (parents) to produce a new design (children). The idea behind crossover is that the new design may be better than both the parents if it takes the best characteristics from each of the parents. Crossover occurs during evolution according to a user definable crossover probability.

A crossover operator that linearly combines two parent designs to produce two new offspring according to the following equations [18]:

$$\text{Offspring 1} = a * \text{Parent 1} + (1 - a) * \text{Parent 2}$$

$$\text{Offspring 2} = (1 - a) * \text{Parent 1} + a * \text{Parent 2}$$

Consider the following two parents (each consisting of four floating genes) which have been selected for crossover:

$$\text{Parent 1: } (0.3)(1.4)(0.2)(7.4)$$

$$\text{Parent 2: } (0.5)(4.5)(0.1)(5.6)$$

If $a = 0.7$, the following two offspring would be produced:

$$\text{Offspring 1} = (0.36)(2.33)(0.17)(6.86)$$

$$\text{Offspring 2} = (0.402)(2.981)(0.149)(6.842)$$

where, $a =$ crossover probability defined by the user during optimization setup

Based on the probability of crossover, the number of design points are chosen for crossover. A lower probability of crossover means the parents are copied directly in the new population. A higher probability is recommended for exploration of diverse design points within the design space.

4.3.5 Mutation

Mutation alters one or more parameter values in a design from its initial state. This can result in entirely new parameter values being added to the parameter pool. With these new parameter

values, the genetic algorithm may be able to arrive at a better solution than was previously possible. Mutation is an important part of the genetic search, as it helps to prevent the population from stagnating at any local optima. Mutation occurs during evolution according to a user-defined mutation probability. For continuous parameters, a polynomial mutation operator is applied to implement mutation.

$$C = P + (UpperBound - LowerBound) \delta$$

where C is the child, P is the Parent, and δ is a small variation calculated from a polynomial distribution

Designing a latent heat energy storage system will require the design to be light-weight and fast responsive. Thus, the objective of this optimization study was to minimize the *CFD melt time* of the PCM and, also minimize the *Weight of the capsule*. Based on a general understanding of the system, these two objectives are contradictory. Thus, we cannot obtain a single optimum solution. Instead we will have a population of optimal solutions defined as the pareto optimal solutions. This is called Multi-objective Optimization.

4.4 Multi-objective optimization

In case of multi-objective optimization, generally, designs that improve one objective worsen another objective. For example, in case of cylindrical capsule filled with PCM. To reduce the weight, wall thickness of the tube needs to be reduced. But this increases the ID of the tube and hence the quantity of the PCM, and consequently the melt time of the PCM. Thus, reducing the weight results in increase in the melt time and vice versa. Hence, in case of multi objective optimization, there is no clear optimum solution. Instead there are many optimal solutions that form a pareto front. The aim of a multi-objective optimization is to improve this pareto front.

4.4.1 Pareto dominance

Considering the contradictory nature of the multiple objectives (improving one leads to worsening the other), ranking these objectives according to one single criterion is not possible. Thus, rather than using a ranking method for the selection process, a pareto front is used for selection. Design

points that form this pareto front are then passed on for crossover and mutation in the Genetic Algorithm process. Pareto dominance is used to generate this pareto front.

After the initial design points (in the 1st iteration/generation) or design points per iteration (in iterations/generations after the 1st) are generated and updated using either the initial sampling process or crossover and mutation respectively, they are segregated into a non-dominated set or a dominated set [29].

For simplicity, let's assume there are two points A and B which belong to the non-dominated set and the dominated set respectively. Point A is defined as a non-dominated design point if

1. it is no worse than a design point B in all objectives, and
2. it is strictly better than a design point B in at least one objective

In case of multi-objective optimization, the non-dominated set of design points is used to generate a pareto front. This pareto front is then further used for reproduction, crossover and mutation to explore the design space to find an optimum pareto front.

A flow illustrating the optimization process for a single objective is shown in the fig. ANSYS Design Exploration within ANSYS Workbench software was used for optimization in this work. The setup used for optimization problem is given in table 8.

Table 8 Optimization algorithm details (ANSYS Design Explorer)

Method Selection	Manual
Method Name	MOGA
Type of Initial Sampling	Screening
Number of Initial Samples	2000
Number of Samples Per Iteration	400
Maximum Allowable Pareto Percentage	70
Convergence Stability Percentage	2
Maximum Number of Iterations	20
Mutation Probability	0.2
Crossover Probability	0.98
Maximum Number of Candidates	10

Chapter 5 Results

Optimization of the cylindrical capsule is done for two objectives, melt time of the PCM and weight of the cylindrical capsule. Outer diameter and wall thickness of the capsule were used as input parameters. Heat capacity of the capsule was used as a constraint in constrained optimization.

Four different types of optimization were studied viz. unconstrained single and multi-objective optimization, constrained single and multi-objective optimization. Six cases were used to demonstrate this methodology.

5.1 Case 1: Optimization of Weight (Unconstrained)

The objective is to minimize the weight of the cylindrical capsule without any constraints. Fig 11 shows a plot of *Weight of the capsule vs CFD Melt time*. The plot clearly shows that when optimizing for just one objective, one single optimum solution exists. Also, the optimization process starts with higher values of the objective function i.e. weight of the capsule and converges to a minimum value of 5.3398 g. The results of this case is given in the table 9.

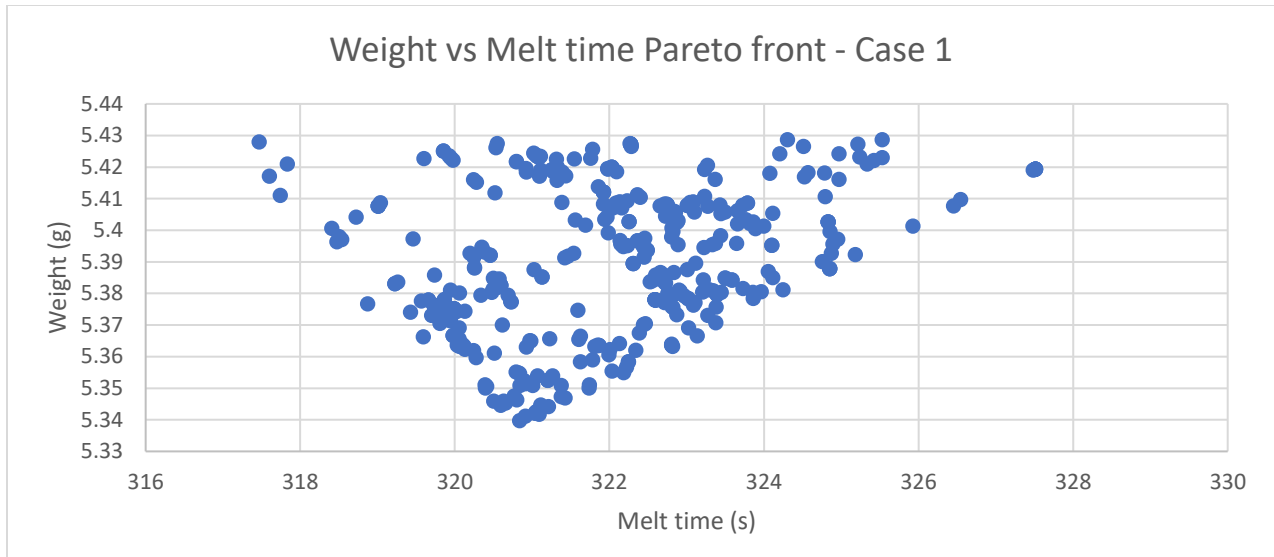


Figure 11 Weight vs Melt time Pareto front - Case 1

Table 9 Results Case 1

OD (mm)	WT (mm)	Melt time (s)	Weight (kg)	Heat capacity (KJ)
6.003	0.500	321	5.3398	1.210

5.2 Case 2: Optimization of Melt time (Unconstrained)

The objective is to minimize the melt time of the PCM without any constraint. Fig. 12 shows a Pareto front of Weight of the capsule vs the CFD Melt time which shows that the optimization process starts with a higher value of the objective i.e CFD Melt time of PCM and clearly indicates convergence of the solution to the lowest Melt time of 122.427 s. The result of this case is shown in the table 10.

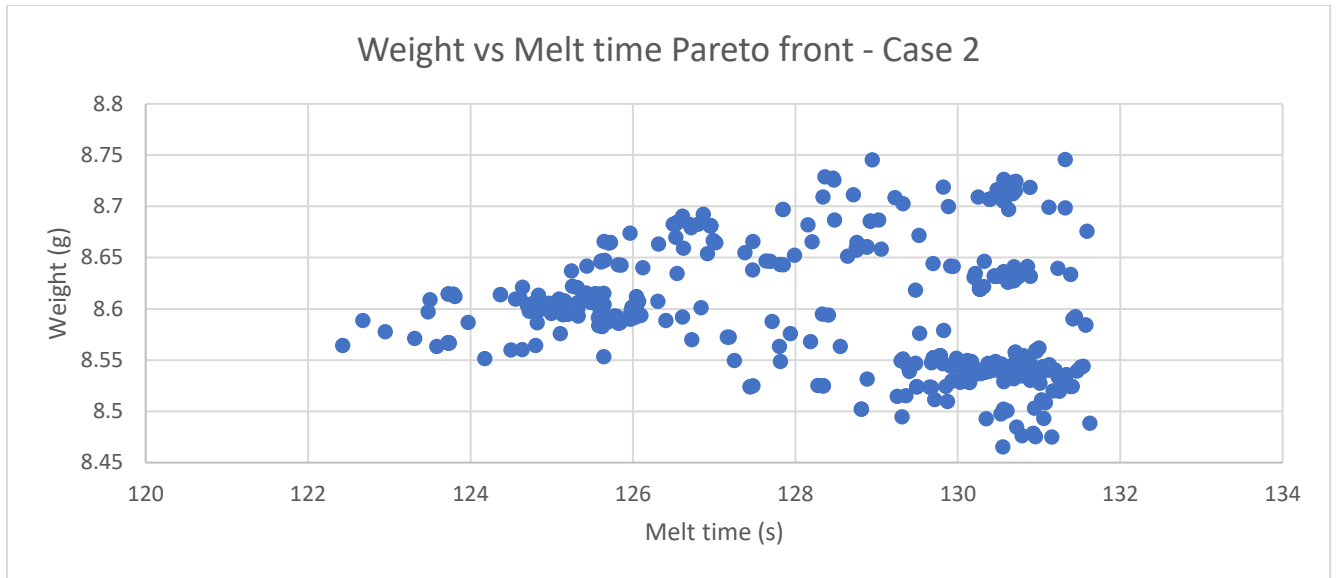


Figure 12 Weight vs Melt time Pareto front - Case 2

Table 10 Results - Case 2

OD (mm)	WT (mm)	Melt time (s)	Weight (kg)	Heat Capacity (KJ)
6.0129	1.498	122.427	8.5642	1.3134

5.3 Case 3: Multi objective optimization of Weight vs Melt time without constraint

The objective is to minimize both melt time and weight simultaneously without any constraints. **N** iterations and evaluations were performed to reach the optimal pareto front. The fig. 13 shows evolution of the weight-melt time pareto front over generations of the genetic algorithm process. Since there is no single “optimum” solution to the multi-objective optimization of the two contradictory objectives, Weight of the capsule and the CFD Melt time, there is no single “optimum” solution, a pareto front is obtained. The optimization process starts with a pareto front with higher values of the Weight of capsule and CFD Melt time of PCM. As the process continues, it starts converging to a pareto front with lower values of Weight of capsule and CFD Melt time of PCM. Fig. 14 shows the final pareto front which is also seen in fig. 13 as “Pareto front 1”.

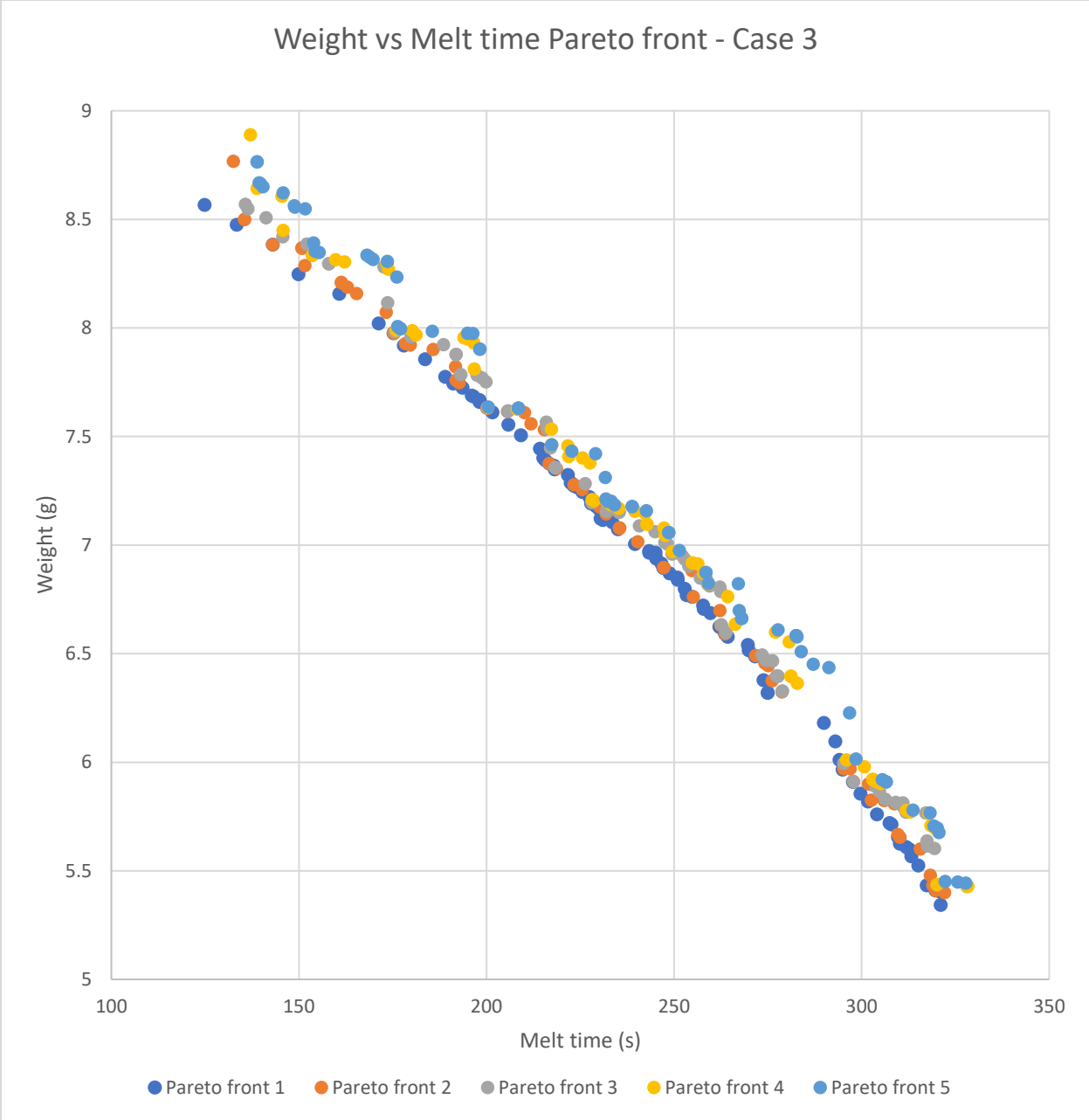


Figure 13 Weight vs Melt time Pareto front - Case 3

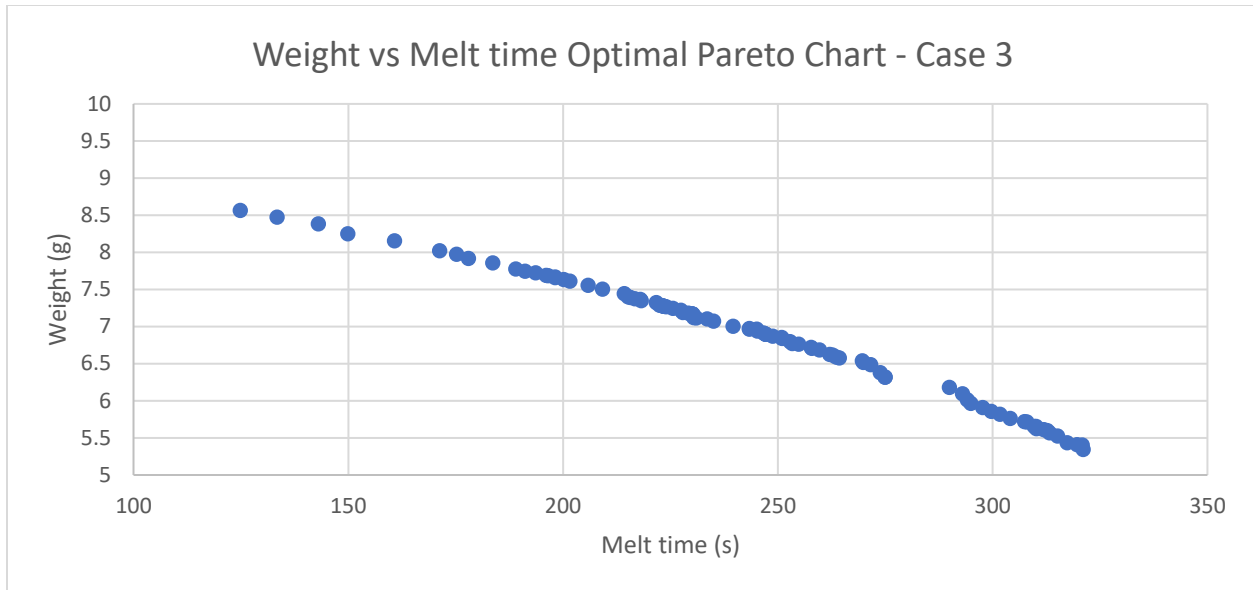


Figure 14 Weight vs Melt Time Optimal Pareto chart - Case 3

5.4 Case 4: Optimization of Weight (Heat Capacity as constraint)

This case was chosen to show how constrained optimization is different from the unconstrained optimization cases. The objective is to minimize the weight of the capsule within constraints of Heat capacity of 9 kJ – 10 kJ. The value of constraint is chosen arbitrarily. Fig. 15 shows the history of convergence of heat capacity over generations of the optimization process. The chart shows that initially in the first iteration, the search space obtained using crossover and mutation is wider than the constraints of Heat Capacity i.e. 9 kJ to 10 kJ. However, through the selection process, infeasible design points (design points that do not satisfy the constraints), are eliminated. The 2nd iteration starts crossover and mutation with only those design points that satisfy the constraint. As the optimization process progresses, the search space starts converging to the optimal solution. The fig. 16 shows a pareto plot for Case 4. The result of Case 4 is given in table 11.

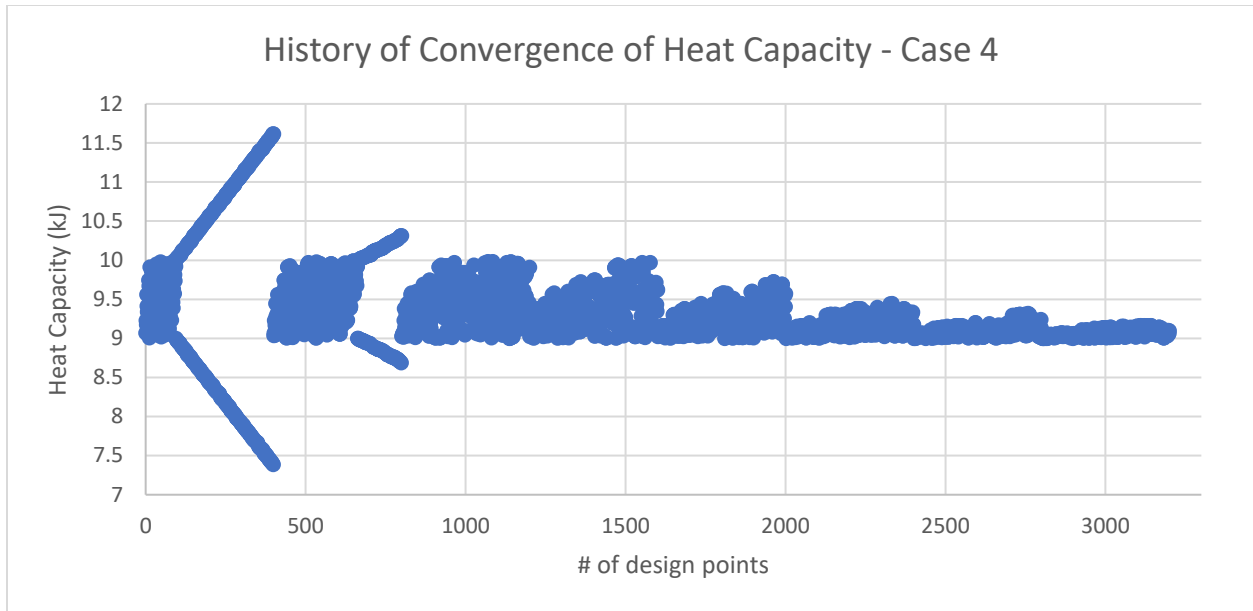


Figure 15 History of Convergence of Heat Capacity - Case 4

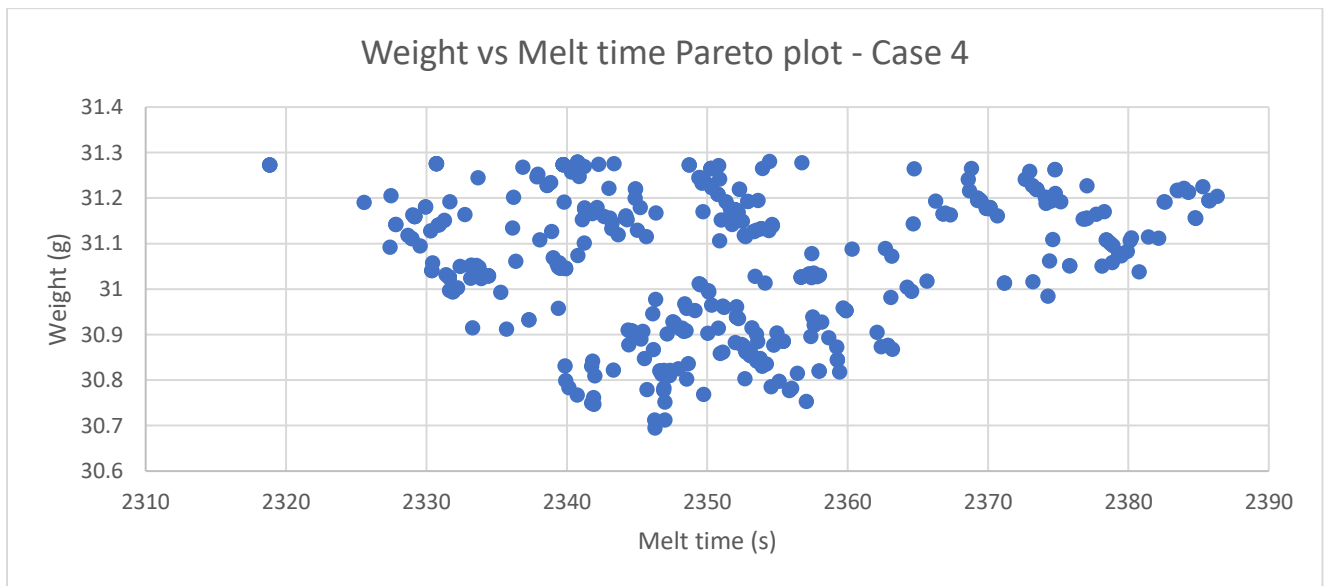


Figure 16 Weight vs Melt time Pareto Plot – Case 4

Table 11 Results - Case 4

OD (mm)	WT (mm)	Melt time (s)	Weight (g)	Heat Capacity (KJ)
16.66705	0.505006	2346.273	30.69459	9.005702

5.5 Case 5: Optimization of Melt time (Heat Capacity as constraint)

The objective is to minimize the *CFD Melt time* such that the input parameters combine to satisfy 9 kJ – 10 kJ heat capacity constraint. The fig. 17 shows a pareto plot of *Weight of capsule vs CFD Melt time*. The results of the Case 5 are given in table 12.

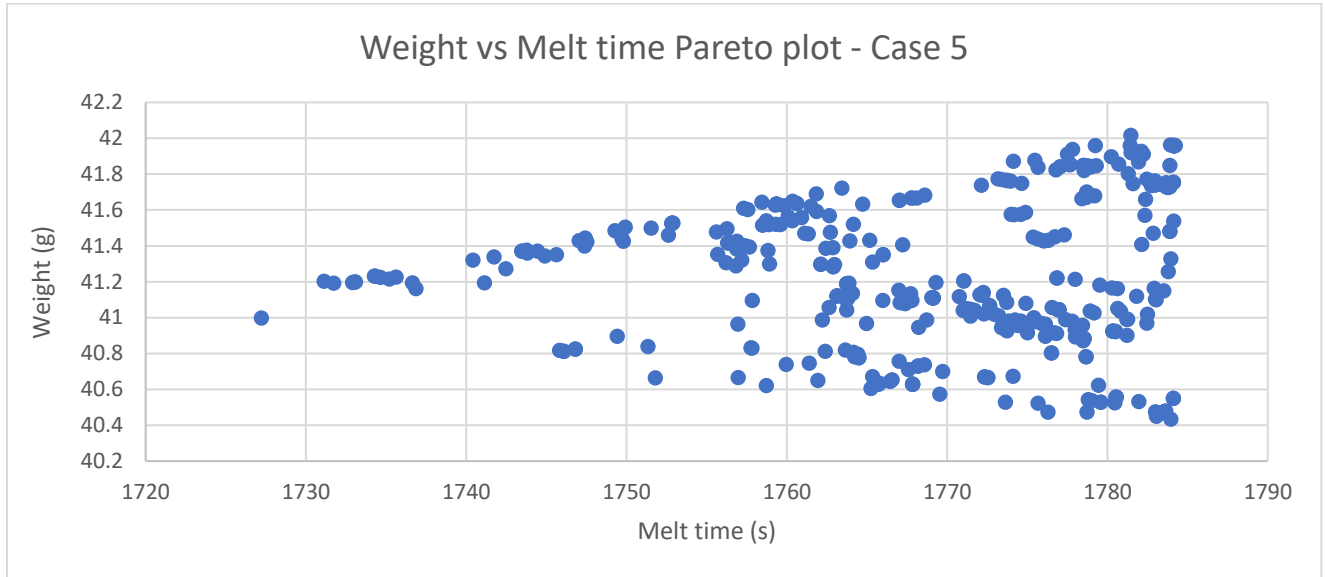


Figure 17 Weight vs Melt time Pareto plot - Case 5

Table 12 Results - Case 5

OD (mm)	WT (mm)	Melt time (s)	Weight (g)	Heat Capacity (KJ)
16.34298	1.493361	1727.224	40.99778	9.01393

5.6 Case 6: Multi objective optimization of Weight vs Melt time (Heat Capacity constraint)

The objective is to find optimal pareto solutions for *Weight of capsule vs CFD Melt time* of the PCM in a constrained setup. Fig. 20 shows a progression of the optimal pareto front over 5 generations. The objective is to optimize for *Weight of capsule* and *CFD Melt time* simultaneously which makes this case a multi-objective problem. Since the two objectives are contradictory, a single optimal solution to the problem does not exist. Thus, fig. 18 shows a tradeoff chart (pareto plot) for Case 6. Fig. 19 show a comparison between the pareto plots for the constrained (Case 6) and unconstrained (Case 3) optimization problems. Fig. 21 to fig. 25 also shows convergence history for Heat capacity, Weight of the Capsule, CFD Melt time, OD and Wall thickness respectively.

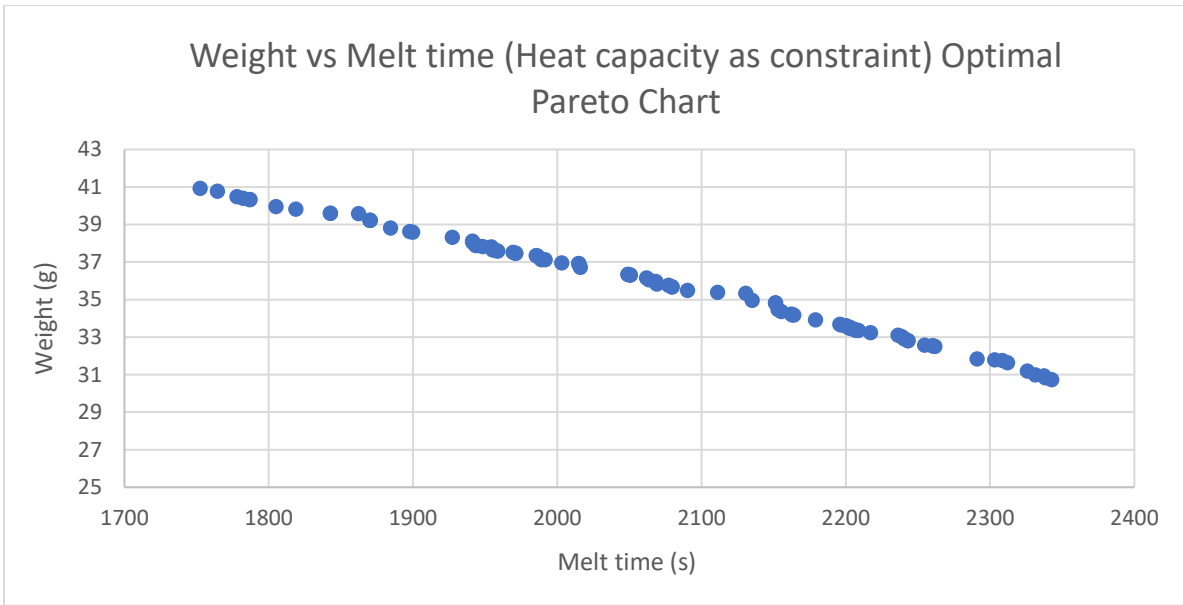


Figure 18 Weight vs Melt time Optimal Pareto Chart - Case 6

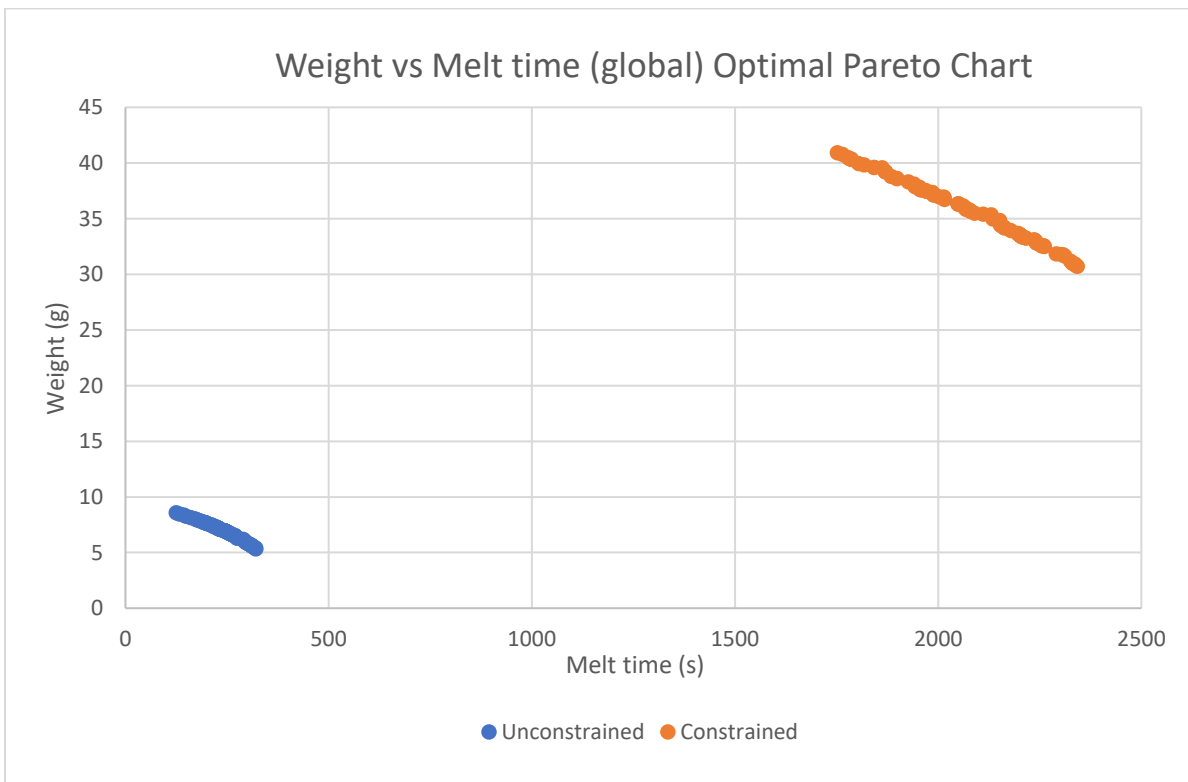


Figure 19 Weight vs Melt Time Global Optimal Pareto Chart

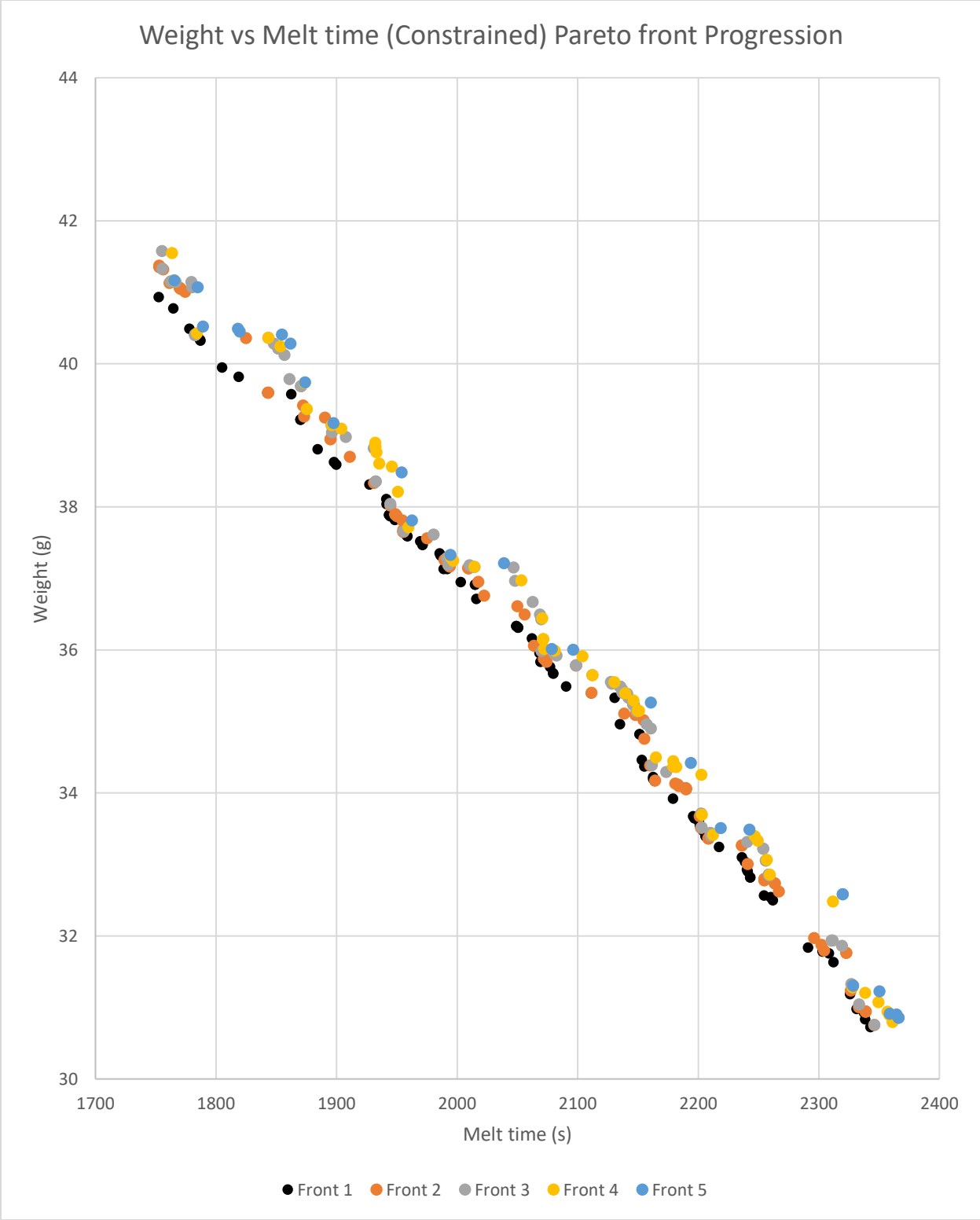


Figure 20 Weight vs Melt time Pareto front progression

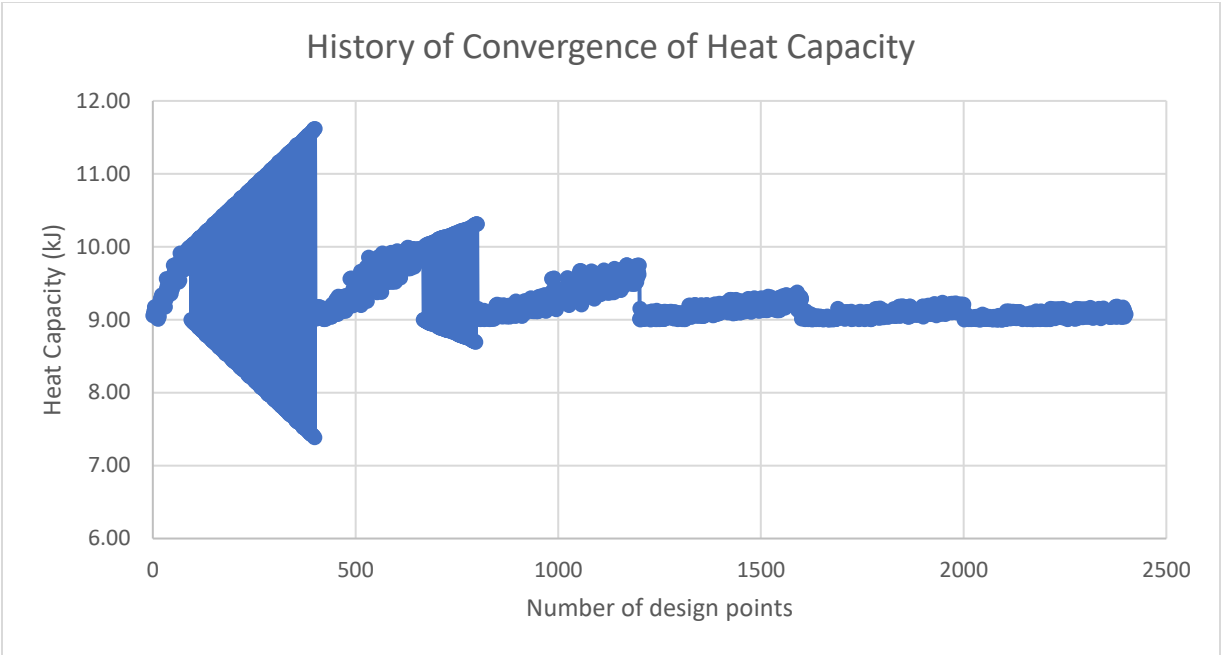


Figure 21 History of Convergence of Heat Capacity - Case 6

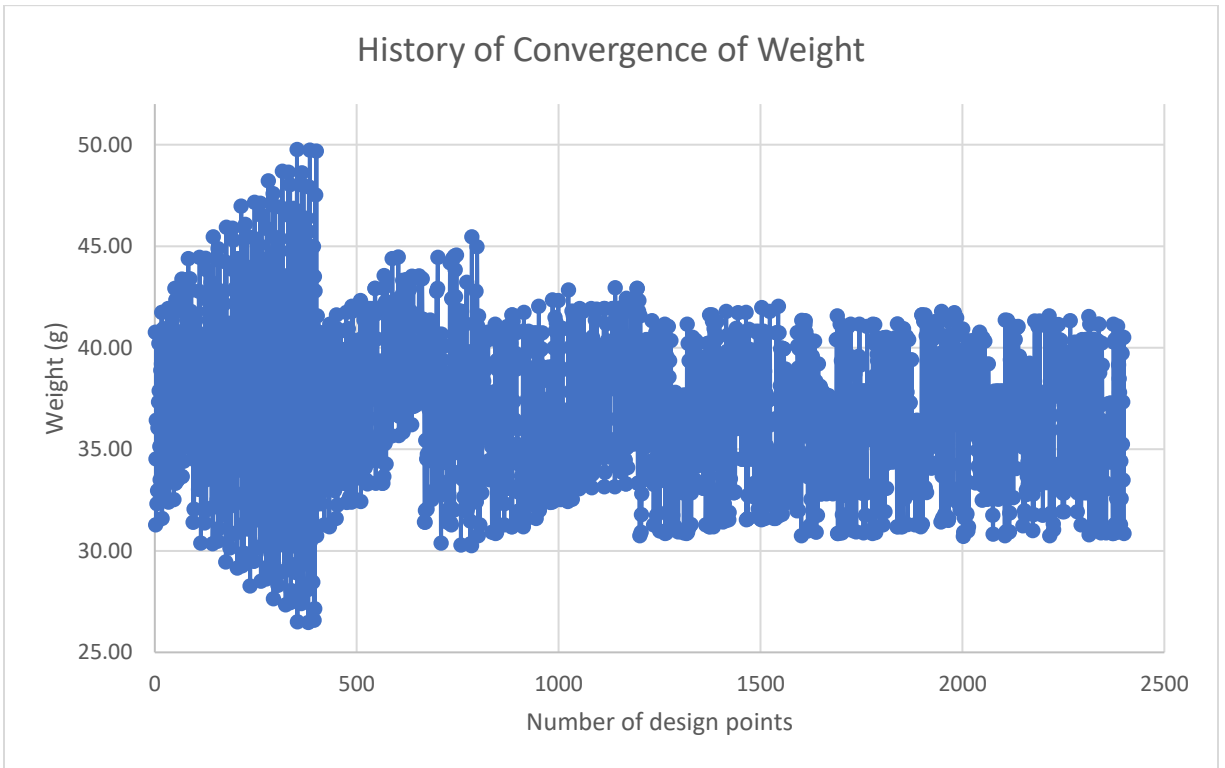


Figure 22 History of Convergence of Weight

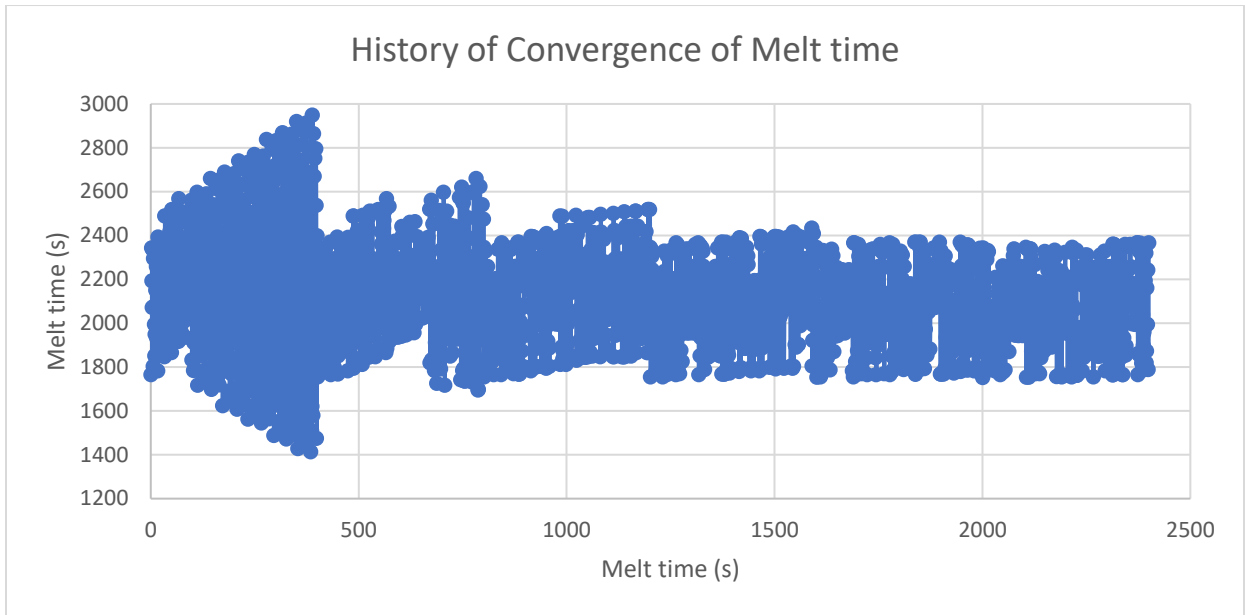


Figure 23 History of Convergence of Melt time - Case 6

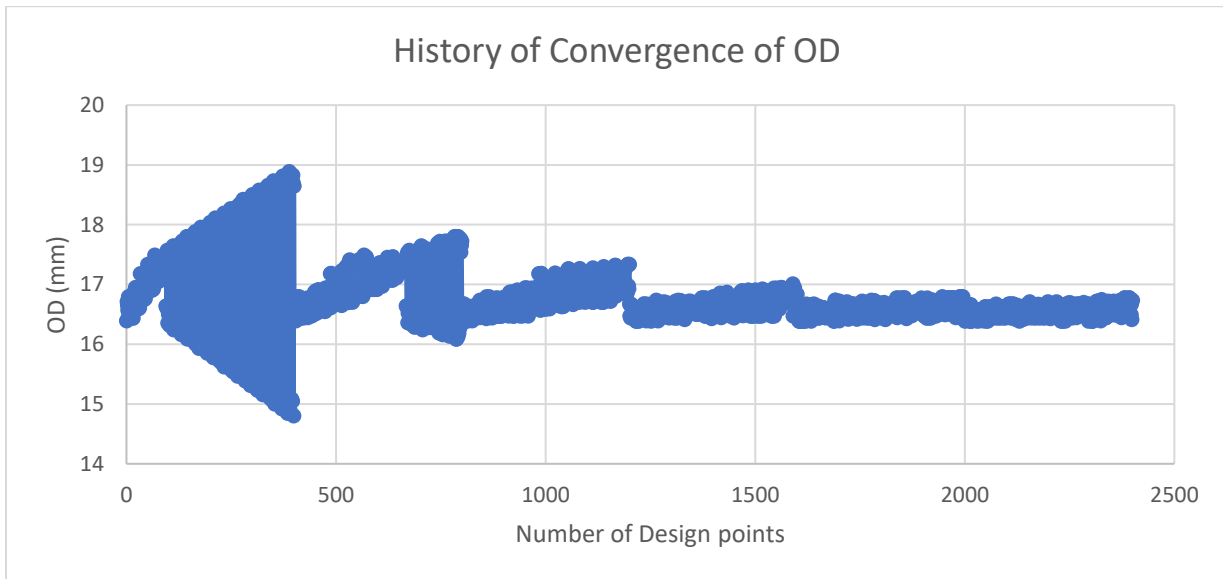


Figure 24 History of Convergence of OD

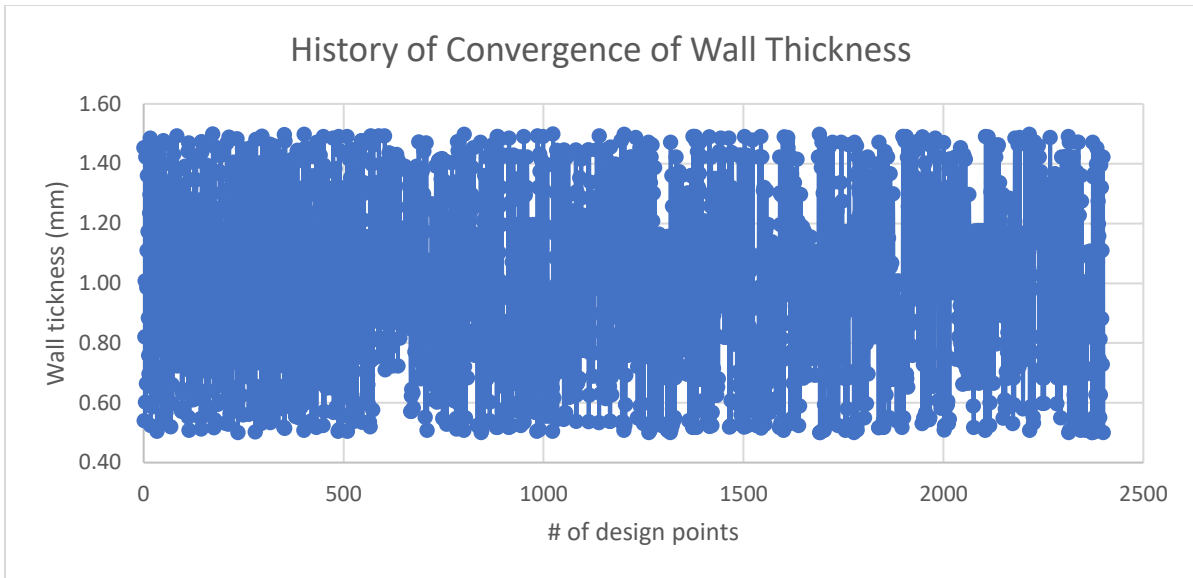


Figure 25 History of Convergence of Wall Thickness - Case 6

Chapter 6 Conclusion

This work presents the use of Phase Change Material (PCM) as a medium of thermal energy storage. A cylindrical capsule was used as a containment vessel for the PCM and heat transfer for this setup was analyzed using numerical simulations (Computational Fluid Dynamics, CFD). The CFD model for melting of PCM inside a cylindrical capsule placed horizontally in crossflow of hot air was studied. This study yielded good agreements with experimental results. Central Composite method was used as a Design of Experiments (DoE) type which required 9 CFD simulations to approximate the 2nd order polynomial relationship between the input parameters and output responses. The regression models using the DoE points were used for approximation of the output responses instead of actual CFD simulations. These models facilitated the evaluation of the output responses viz. CFD Melt time of PCM in fractions of seconds instead of days of simulation run time. Genetic (Evolutionary) algorithm was used for optimizing the CFD Melt time and Weight of the capsule. Using the regression models generated with the help of response surface methodology, 6 different cases of optimization were studied, which involved constrained vs unconstrained optimization, and single vs multi-objective optimization. The key result of the current work was the development of design optimization methodology that can be used in a product development to efficiently design a thermal energy storage system or any other heat exchanger device.

6.1 Future scope

The purpose of this work to *demonstrate* a methodology, for design optimization of thermal energy storage devices using CFD, that can minimize the time and resources required in the early stages of product design process. The single cylindrical capsule could be used in multiple configurations like a rod bundle to increase the heat storage capacity of the thermal energy storage system. Such rod bundled PCM heat exchangers can be used in various applications viz. solar energy storage, building HVAC applications, waste heat recovery to name a few. The complexity of the heat exchanger design can be increased by adding more design variables viz. number of tubes,

arrangement of tubes, etc. and output responses (objective functions) viz. pressure drop, cost, etc. This increase of number of design variables increases the difficulties in finding optimum designs with heuristic methods as the required CFD simulations/experiments increases drastically. Thus, increasing the number of design variables will lead to greater possibilities for the use of optimization methodology suggested in this work.

Appendix Software Interfaces

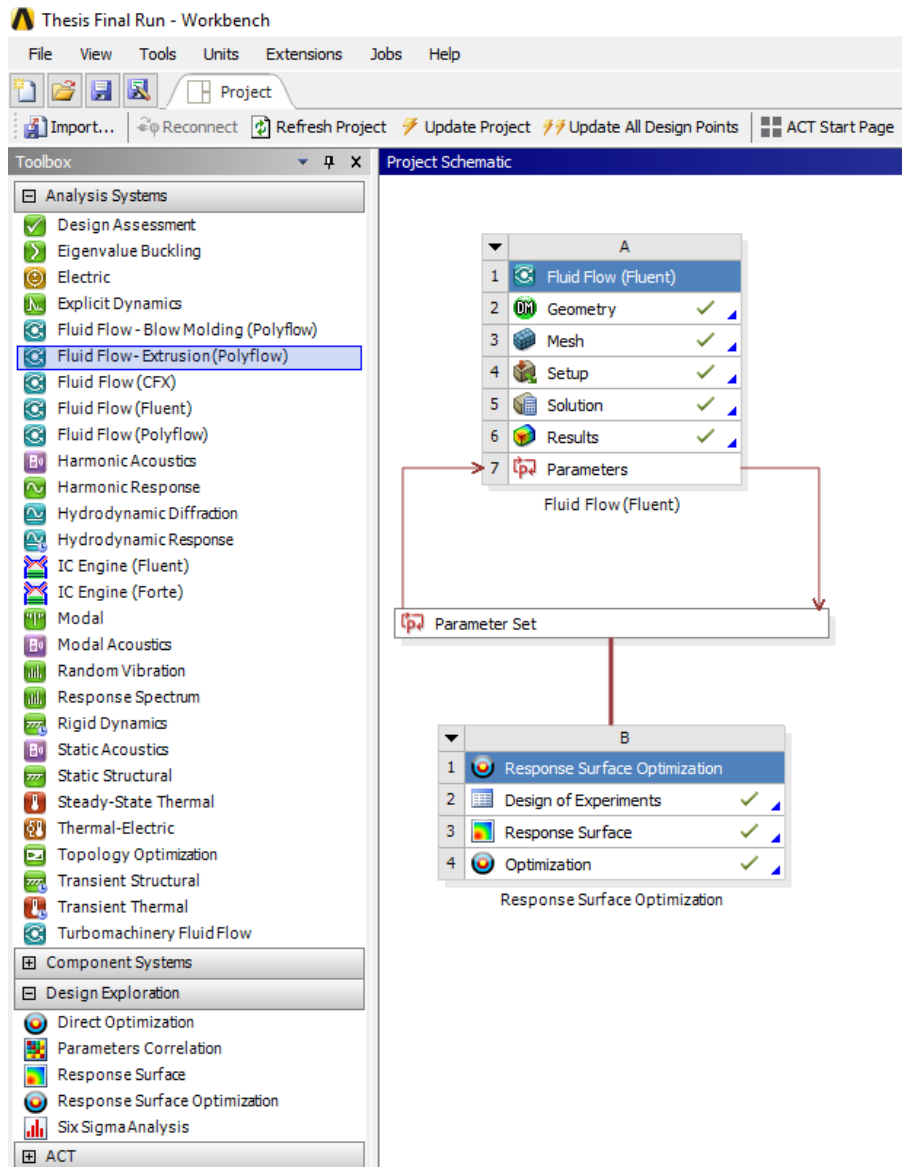


Figure 26 ANSYS Workbench Project Layout

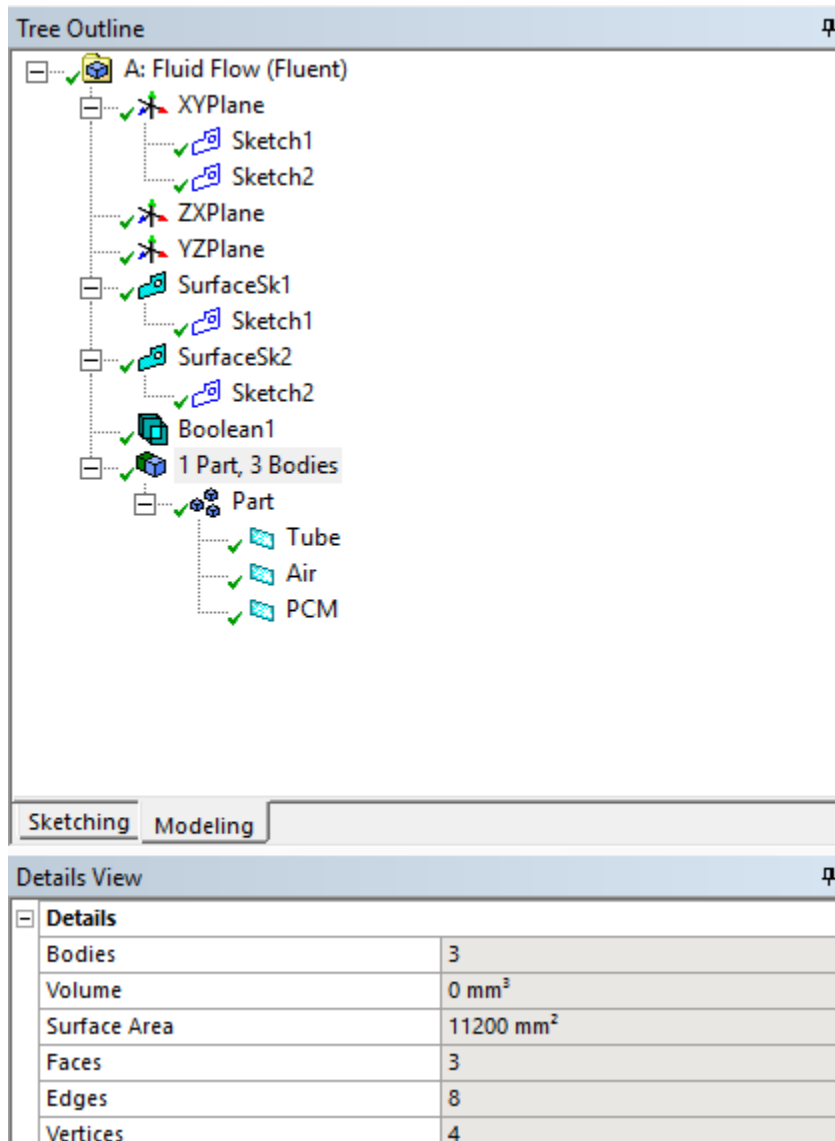


Figure 27 ANSYS Design Modeler Interface

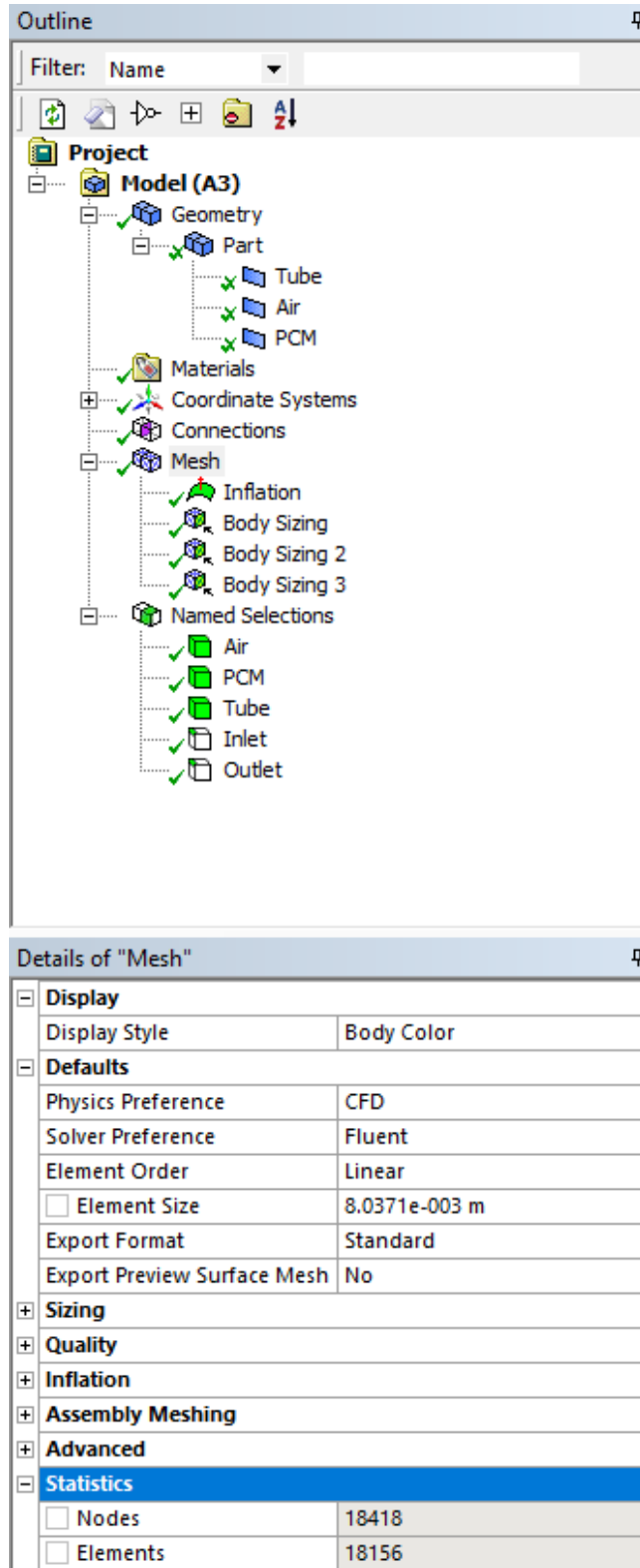


Figure 28 ANSYS Mesher Interface

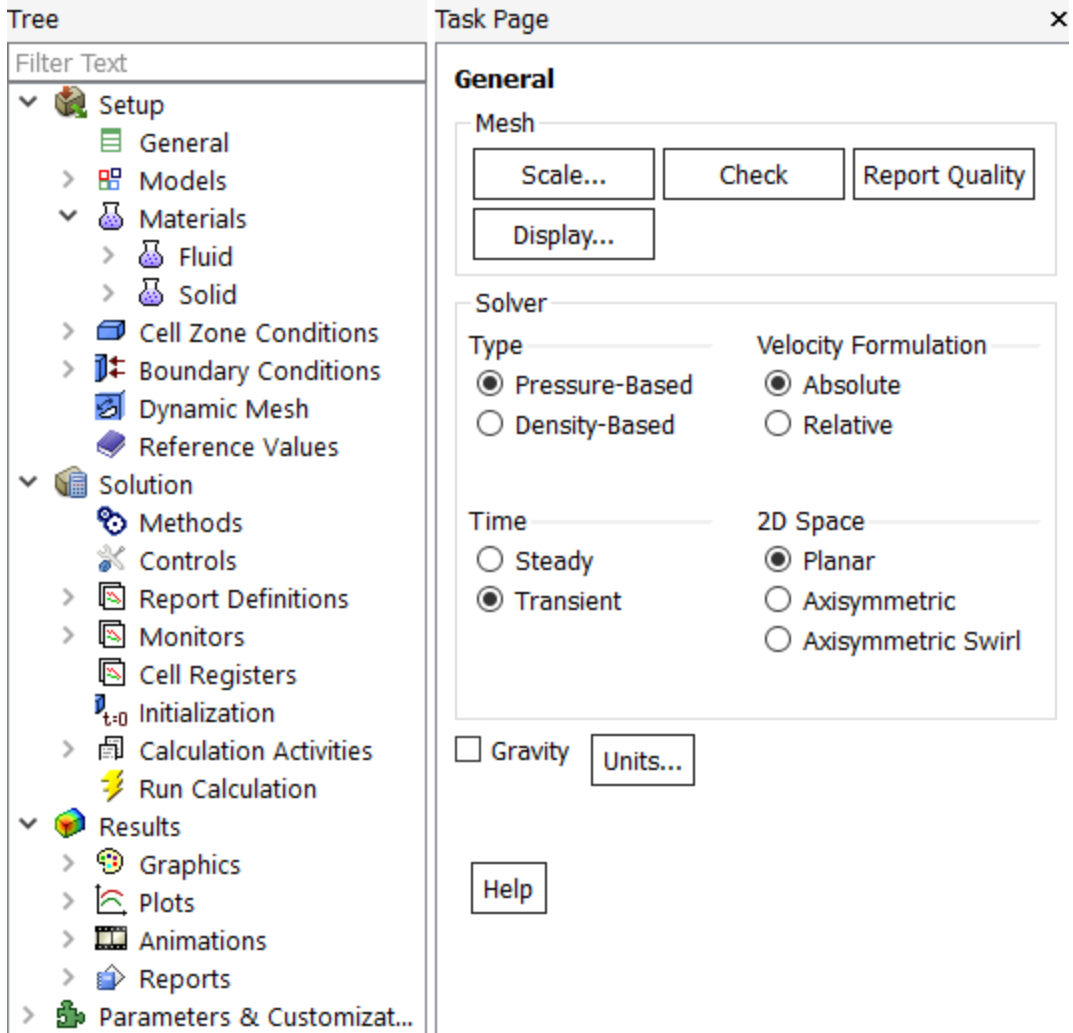


Figure 29 ANSYS FLUENT Interface

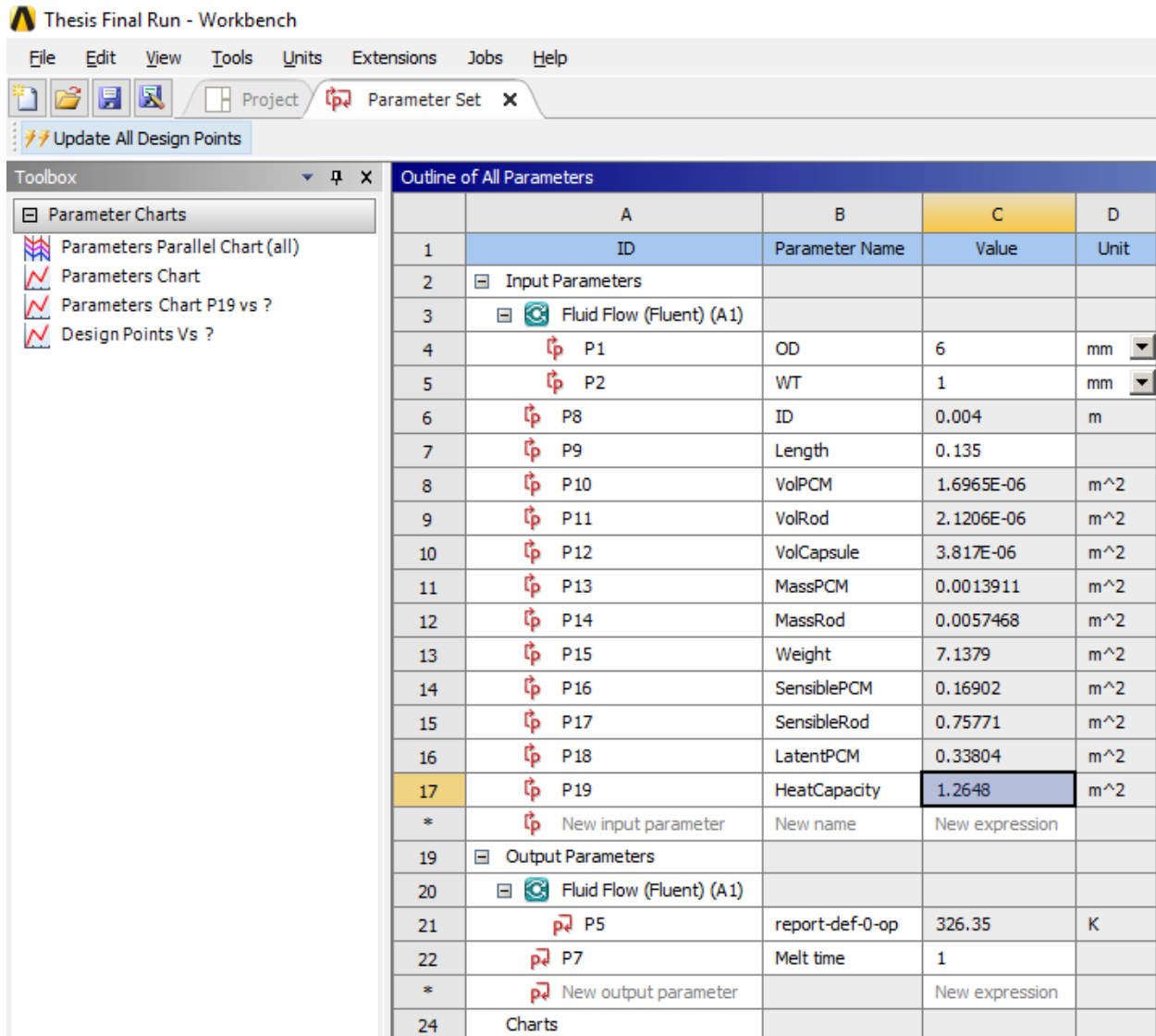


Figure 30 Input and Output Parameter Set

In the Parameter set described above, parameters P1 (OD), and P2 (Wall Thickness) are actual input parameters that are used for DOE component. Parameters P8 – P19 are synthetic parameters obtained using list of formulae from 2.2.5. Parameters P7 (Melt time), P15 (Weight) and P19 (Heat Capacity) are used as Output Parameters. Parameter P5 is redundant.

Outline of Schematic B2: Design of Experiments		
	A	B
1		Enabled
2	Design of Experiments	
3	Input Parameters	
4	Fluid Flow (Fluent) (A1)	
5	P1 - OD	<input checked="" type="checkbox"/>
6	P2 - WT	<input checked="" type="checkbox"/>
7	P9 - Length	<input type="checkbox"/>
8	Output Parameters	
9	Fluid Flow (Fluent) (A1)	
10	P5 - report-def-0-op	
11	P7 - Melt time	
12	P8 - ID	
13	P10 - VolPCM	
14	P11 - VolRod	
15	P12 - VolCapsule	
16	P13 - MassPCM	
17	P14 - MassRod	
18	P15 - Weight	
19	P16 - SensiblePCM	
20	P17 - SensibleRod	
21	P18 - LatentPCM	
22	P19 - HeatCapacity	
23	Charts	
24	Parameters Parallel	
25	Design Points vs Parameter	

Properties of Outline : Design of Experiments		
	A	B
1	Property	Value
2	Design Points	
3	Preserve Design Points After DX Run	<input type="checkbox"/>
4	Failed Design Points Management	
5	Number of Retries	0
6	Design of Experiments	
7	Design of Experiments Type	Central Composite Design
8	Design Type	Auto Defined
9	Design Point Report	
10	Report Image	None

Figure 31 ANSYS Design of Experiments Interface

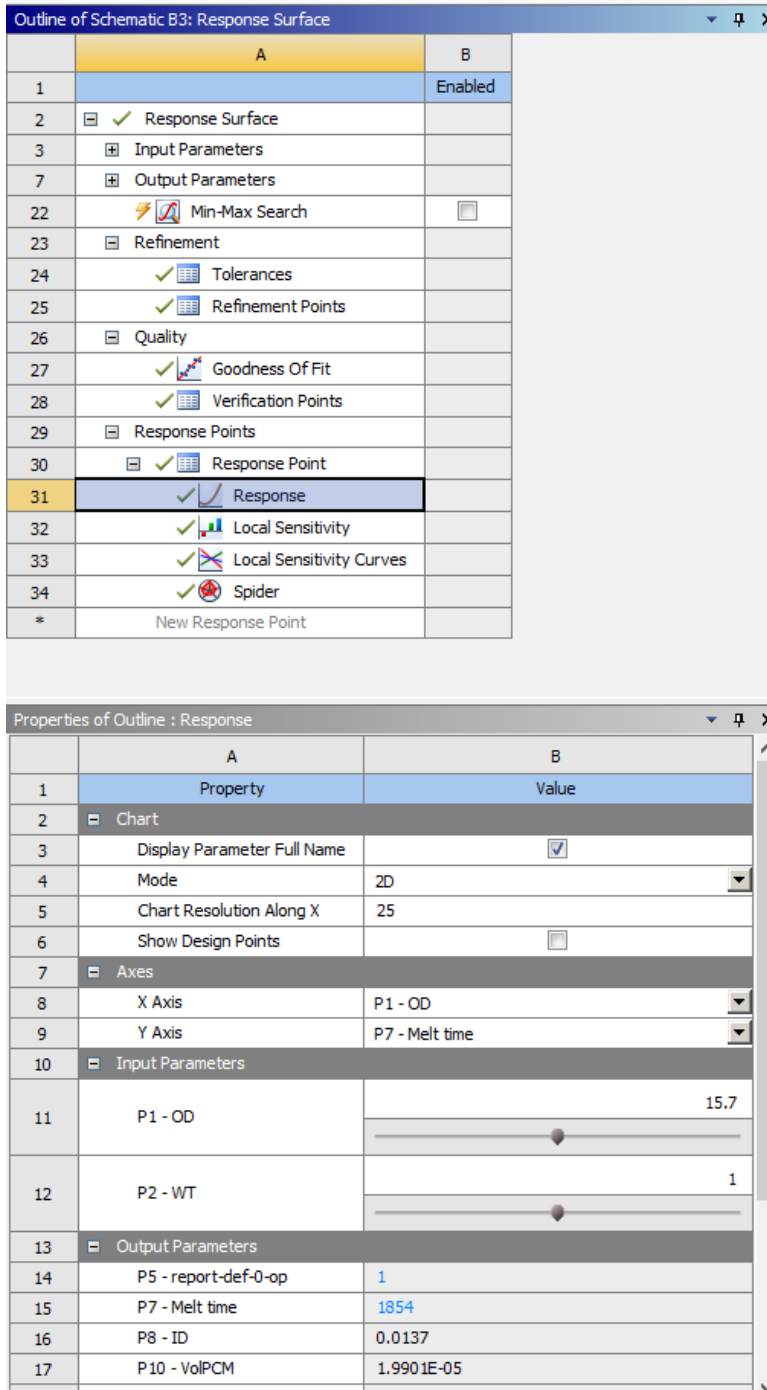


Figure 32 ANSYS Response Surface Interface

Outline of Schematic B4: Optimization			
	A	B	C
1		Enabled	Monitoring
2	✓ Optimization		
3	Objectives and Constraints		
4	Minimize P7		
5	$9 \text{ m}^2 \leq P19 \leq 10 \text{ m}^2$		
6	Domain		
7	Fluid Flow (Fluent) (A1)		
10	Parameter Relationships		
11	✓ Convergence Criteria		
12	Results		
13	✓ Candidate Points		
14	✓ Tradeoff		
15	✓ Samples		
16	✓ Sensitivities		

Properties of Outline A2: Optimization		
	A	B
1	Property	Value
2	Design Points	
3	Preserve Design Points After DX Run	<input type="checkbox"/>
4	Failed Design Points Management	
5	Number of Retries	0
6	Optimization	
7	Method Selection	Manual
8	Method Name	MOGA
9	Estimated Number of Evaluations	9600
10	Verify Candidate Points	<input type="checkbox"/>
11	Number of Initial Samples	2000
12	Number of Samples Per Iteration	400
13	Maximum Allowable Pareto Percentage	70
14	Convergence Stability Percentage	2
15	Maximum Number of Iterations	20
16	Maximum Number of Candidates	10
17	Optimization Status	
18	Converged	Yes
19	Pareto Percentage	0.25

Figure 33 ANSYS Optimization Interface

References

- [1] U.-H. Jung, J.-H. Kim, J.-H. Kim, C.-H. Park, S.-O. Jun and Y.-S. Choi, "Optimum design of diffuser in a small high-speed centrifugal fan using CFD and DOE," *Journal of Mechanical Science and Technology*, vol. 30, no. 3, p. 1171~1184, 2016.
- [2] J.Ortega-Casanova, "Application of CFD on the optimization by response surface methodology of a micromixing unit and its use as a chemical microreactor," *Chemical Engineering & Processing: Process Intensification*, vol. 117, pp. 18-26, 2017.
- [3] S. Lohrasbi, M. G. Bandpy and D. Ganji, "Response surface method optimization of V-shaped fin assisted latent heat thermal energy storage system during discharging process," *Alexandria Engineering Journal*, vol. 55, pp. 2065-2076, 2016.
- [4] R. Hilbert, G. Janiga, R. Baron and D. Thevenin, "Multi-objective shape optimization of a heat exchanger using parallel genetic algorithms," *International Journal of Heat and Mass Transfer*, vol. 49, p. 2567–2577, 2006.
- [5] Z. Ling, Z. Zhang, G. Shi, X. Fang, L. Wang, X. Gao, Y. Fang, T. Xu, S. Wang and X. Liu, "Review on thermal management systems using phase change materials for electronic components, Li-ion batteries and photo voltaic modules," *Renewable and Sustainable Energy Reviews*, vol. 31, pp. 427-438, 2014.
- [6] I. Sarbu and C. Sebarchievici, "A Comprehensive Review of Thermal Energy Storage," *Sustainability*, vol. 10, no. 191, 2018.
- [7] M.Bareiss and H.Beer, "An analytical solution of the heat transfer process during melting of an unfixed solid phase change material inside a horizontal tube," *International Journal of Heat and Mass Transfer*, vol. 27, no. 5, pp. 739-746, May 1984.
- [8] A. Atal, Y. Wang, M. Harsha and S. Sengupta, "Effect of porosity of conducting matrix on a phase change energy storage device," *International Journal of Heat and Mass Transfer*, vol. 93, pp. 9-16, Feb 2016.
- [9] J. J. Maldonado, "Experimental Investigation of the Melting Process inside a Horizontal Cylinder," University of Miami, 1986.
- [10] A. K. Prasad, "Numerical Investigation of Melting Inside A Horizontal Cylinder Including effects of Natural Convection," University of Miami, 1985.

- [11] S. Krajnović, "Aerodynamic optimization of vehicles using computational fluid dynamics and response surface methodology," in *XXI Intl. JUMV Automotive Conference SCIENCE & MOTOR VEHICLES*, Belgrade, 2007.
- [12] A. Sciacovelli, F. Gagliardi and V. Verda, "Maximization of performance of a PCM latent heat storage system with innovative fins," *Applied Energy*, vol. 137, pp. 707-715, 1 January 2015.
- [13] C. P. Hedderich, M. D. Kelleher and G. N. Vanderplaats, "Design and Optimization of Air-cooled heat exchangers," *Journal of Heat Transfer*, vol. 104, pp. 683-690, Nov 1982.
- [14] M. Asadi, Y. Song, B. Sunden and G. Xie, "Economic optimization design of shell-and-tube heat exchangers by a cuckoo-search-algorithm," *Applied Thermal Engineering*, vol. 73, no. 1, pp. 1032-1040, 5 December 2014.
- [15] T. Dominique and J. Gábor, *Optimization and Computational Fluid Dynamics*, Springer, 2008.
- [16] A. A. Godarzi, M. Jalilian, J. Samimi, A. Jokar and M. A. Vesaghi, "Design of a PCM storage system for a solar absorption chiller based on exergoeconomic analysis and genetic algorithm," *International Journal of Refrigeration*, vol. 36, no. 1, pp. 88-101, 1st Jan 2013.
- [17] R. Raud, M. E. Cholette, S. Riahi, F. Bruno, W. Saman, G. Will and T. A. Steinberg, "Design optimization method for tube and fin latent heat thermal energy storage systems," *Energy*, vol. 134, pp. 585-594, September 2017.
- [18] ANSYS, *ANSYS User's guide*.
- [19] H. S. (Deceased) and K. Gersten, *Boundary layer theory*.
- [20] F. White, *Fluid Mechanics*.
- [21] C. Prakash, M. Samonds and A. K. Singhal, "A fixed grid numerical methodology for phase change problems involving a moving heat source," *International Journal of Heat and Mass Transfer*, vol. 30, no. 12, pp. 2690-2694, December 1987.
- [22] V. R. Voller, A. D. Brent and C. Prakash, "The modelling of heat, mass and solute transport in solidification systems," *International Journal of Heat and Mass Transfer*, vol. 32, no. 9, pp. 1719-1731, September 1989.
- [23] V. R. V. a. C. R. Swaminathan, "GENERAL SOURCE-BASED METHOD FOR SOLIDIFICATION PHASE CHANGE," *Numerical Heat Transfer, Part B*, vol. 19, pp. 175-189, 1991.
- [24] D. Montgomery, *Design and Analysis of Experiments*.

- [25] W. S. J. D. a. G. L. Senlin Xiao, "Application of CFD, Taguchi Method, and ANOVA Technique to Optimize Combustion and Emissions in a Light Duty Diesel Engine," *Mathematical Problems in Engineering*, 2014.
- [26] A. A. A. R. a. W. M. A. W. D. Anam Asghar, "A Comparison of Central Composite Design and Taguchi Method for Optimizing Fenton Process," *The Scientific World Journal*, 2014.
- [27] G. N. Vanderplaats, Numerical optimization techniques for engineering design with applications, McGraw-Hill Book Company, 1984.
- [28] G. N. V. a. P. J. M. C. M. Johnson, "Marine Condenser Design Using Numerical Optimization," *Journal of Mechanical Design*, vol. 102, no. 3, pp. 469-475, 1980.
- [29] K. Deb, Multi-Objective optimization using Evolutionary algorithms, 2001.
- [30] M.Hatami, M.Jafaryar, D.D.Ganji and M.Gorji-Bandpaya, "Optimization of finned-tube heat exchangers for diesel exhaust waste heat recovery using CFD and CCD techniques," *International Communications in Heat and Mass Transfer*, vol. 57, pp. 254-263, October 2014.